

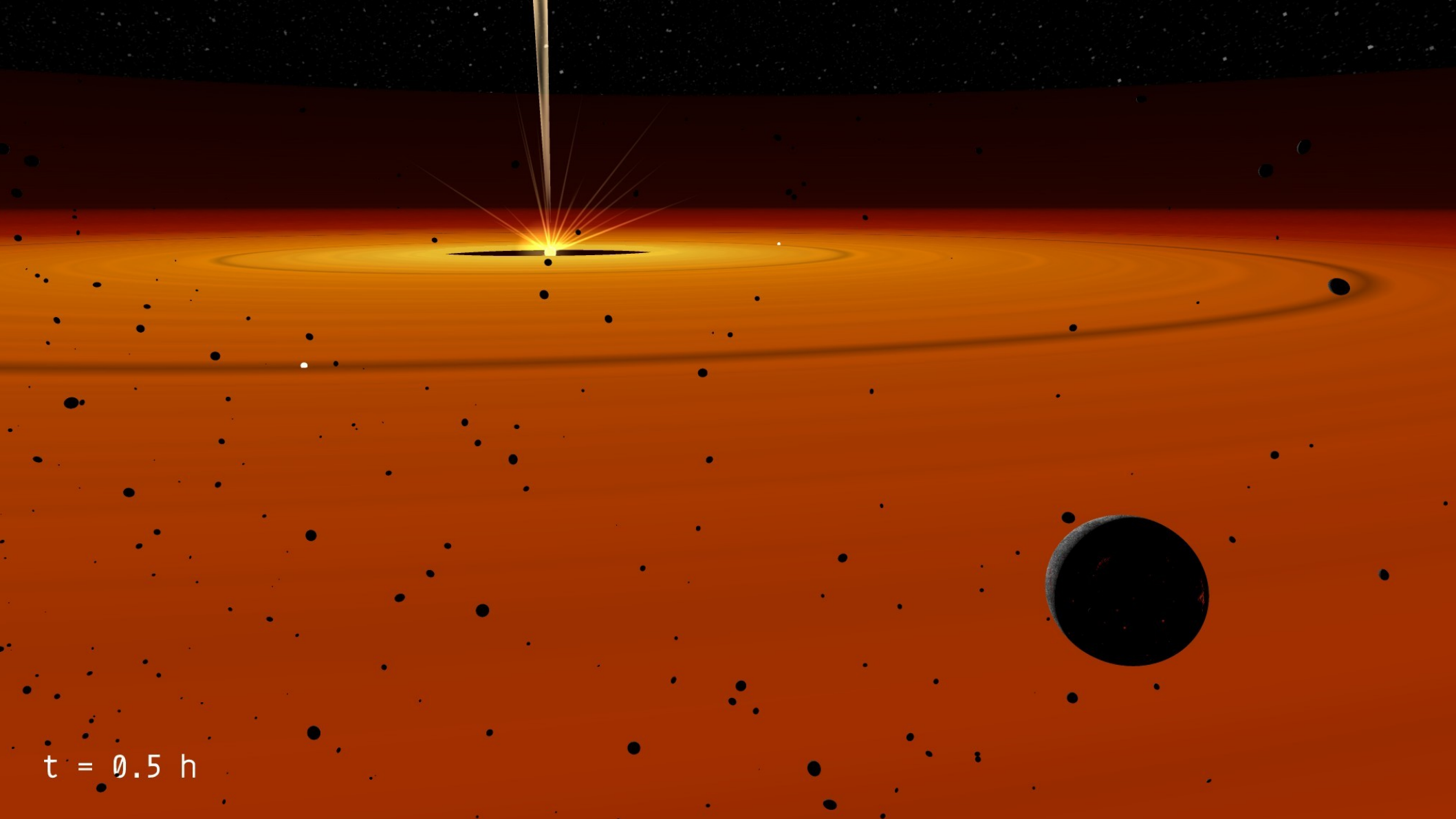
Co víme o vzniku Měsíce a Země?

(resp. nevíme)





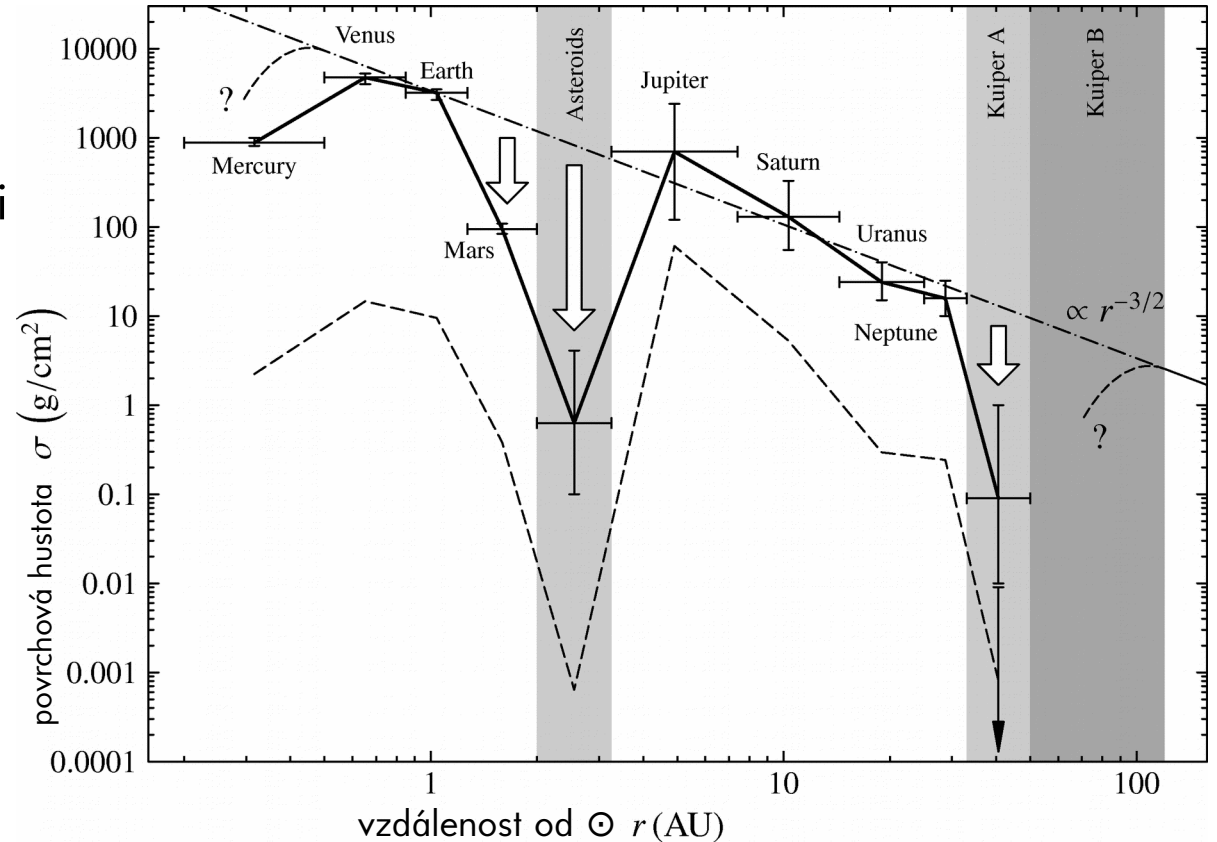
+



$t = 0.5 \text{ h}$

Hayashi (1981) ← viz ADS

- místní materiál...
- ... slunečního složení
- mlhovina minimální hmotnosti
- $\sigma_{\text{MMSN}} = 1700 \text{ g/cm}^2 (r/1 \text{ au})^{-3/2}$



Wetherill (1990)

tribution was quantitatively identified by Safronov (e.g. Safronov 1969) and later developed further by others (Nakagawa et al 1983, Wetherill & Stewart 1989). During the growth of planetesimals into embryos, the growing planetesimals will be sufficiently closely packed to permit collisions between them, a necessary condition for their growth and merger. Calculations of this stage of growth indicate that bodies as large as 10^{26} g can form in $\sim 10^5$ yr.

The present total mass of the terrestrial planet region is 1.18×10^{28} g, of which 51% is in the Earth-Moon system. Therefore, the growth of the Earth and terrestrial planets would require the merger of ~ 100 10^{26} -g planetary embryos. These larger preplanetary bodies will usually be more distant from one another, the rate of growth will slow down, and this final stage of terrestrial planet growth will require 10^7 – 10^8 yr for its completion, probably long after the loss of the gaseous solar nebula in $\lesssim 3 \times 10^6$ yr. This stage of growth is likely to be characterized by the emergence, after $\sim 5 \times 10^6$ yr, of the dominant embryos of the two large terrestrial planets, Earth and Venus, in orbits of relatively low eccentricity and inclination. As a result of gravitational perturbations associated with close encounters of the smaller 10^{26} – 10^{27} -g embryos with Earth and Venus, the remainder of the material will probably be found in more eccentric orbits ($e \sim 0.1$ – 0.3) that span the terrestrial planet region, eliminating local “feeding zones” for each planet. Final accumulation of Earth and Venus then includes “giant impacts,” collisions with residual smaller planet-size embryos. Such impacts have been associated with special events in terrestrial planet history, such as the formation of the Moon (reviewed by Stevenson 1987), the loss of Mercury’s silicate mantle (Wetherill 1988, Cameron et al 1988, Vityazev et al 1988), and the loss of the Earth’s original atmosphere (Cameron 1983).

The same model must account, in a natural way, for the mechanism and

planetesimály na embrya

tj. velikost Měsíce

10^5 let

poslední fáze 10^7 až 10^8 let
mlhovina $< 3 \cdot 10^6$ let

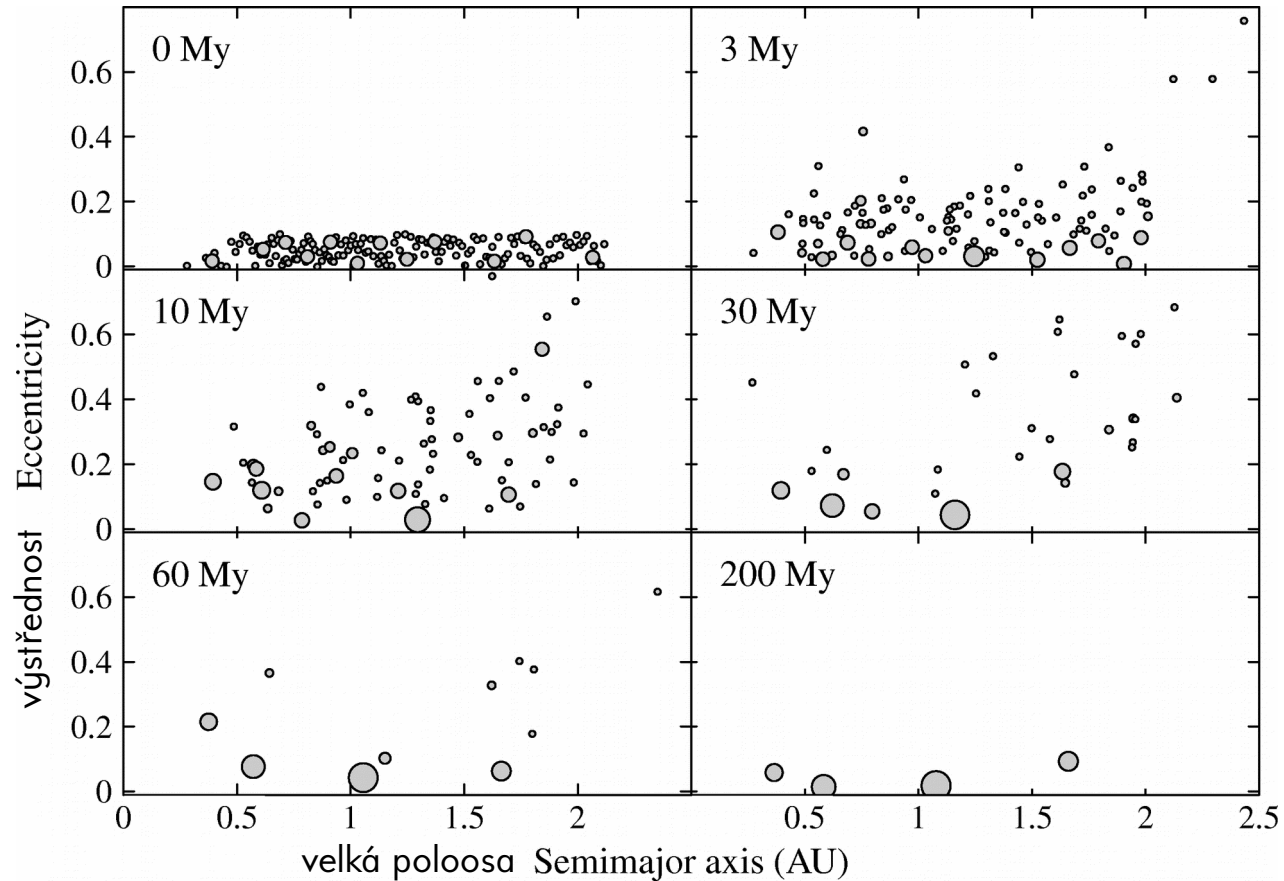
zbývající
na excentrických dráhách

velké impaky

vznik Měsíce
odtržení pláště Merkuru

Chambers & Wetherill (1998)

- N-částicový model
- izolovaná hmotnost
- časová škála s. 10^8 let
- (bez plynu)



Hansen (2009)

- oříznutý disk nebo **mezikruží** 0.7-1 au
- malý Mars!
- dtto Merkur (1)
- velká mezera V.-Z.
- tlumení srážkami (Deienno et al. 2019), dtto

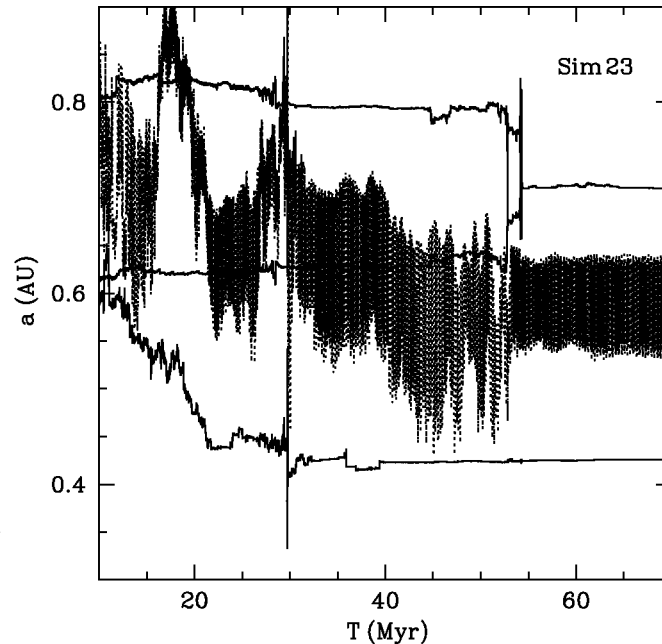


Figure 5. Three solid lines show the temporal evolution of the semi-major axis for the Mercury analog and the two bodies which eventually combine to form the Venus analog. The dotted line shows the apastron of the Mercury analog. We see that the Mercury analogue is pushed inward by scattering off the innermost of the two Venus progenitors. Eventually, a late impact (54 Myr) results in the merger of the two roughly equal mass bodies to form the final Venus analog. The collision product has a final semi-major axis intermediate between those of the progenitors, and the result is that the Mercury analog is no longer dynamically coupled to the outer bodies.

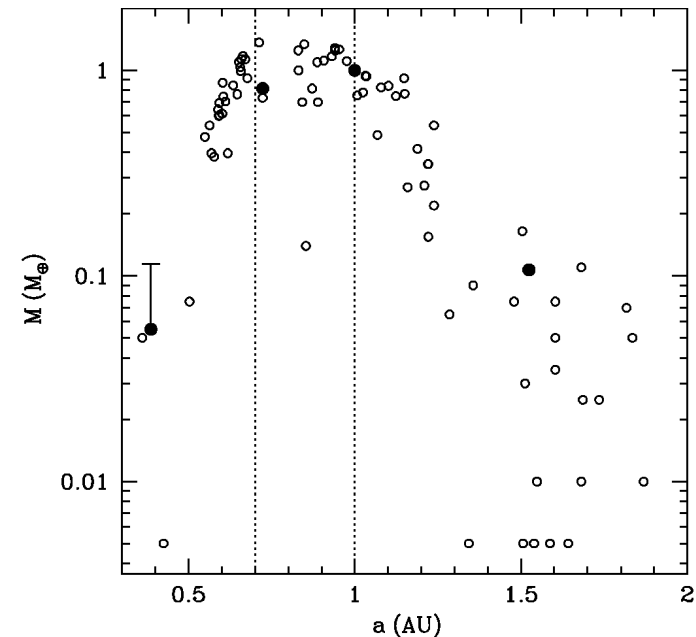
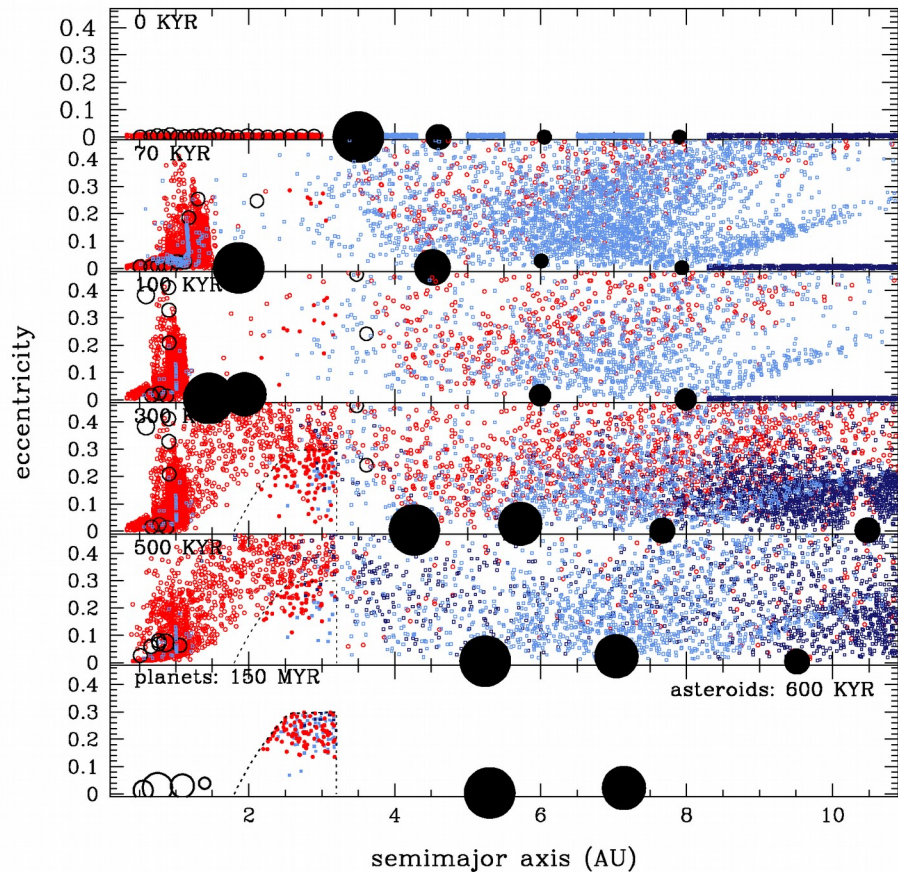


Figure 1. Open circles represent the distribution of bodies remaining in our simulations, while the solid points are the four observed solar system planets. The vertical error bar for Mercury indicates the possible original larger mass if it originally had the same iron content as the other terrestrial planets. The vertical dotted lines indicate the edges of the original annulus.

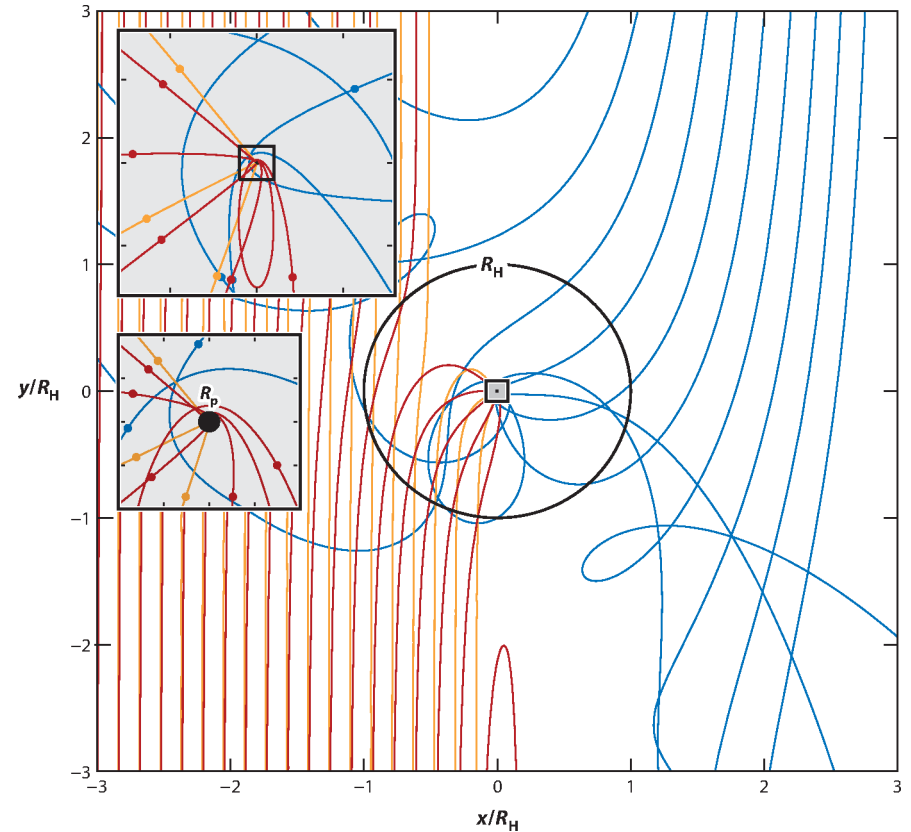
Walsh et al. (2011)

- Jupiter & Saturn, migrace typu II
- 'otočená' rezonancí 2:1, překryv mezer
- vnější okraj oříznut; vnitřní?
- malý Mars ($0.1 M_E$)
- oblíbený model v meteoritické k.



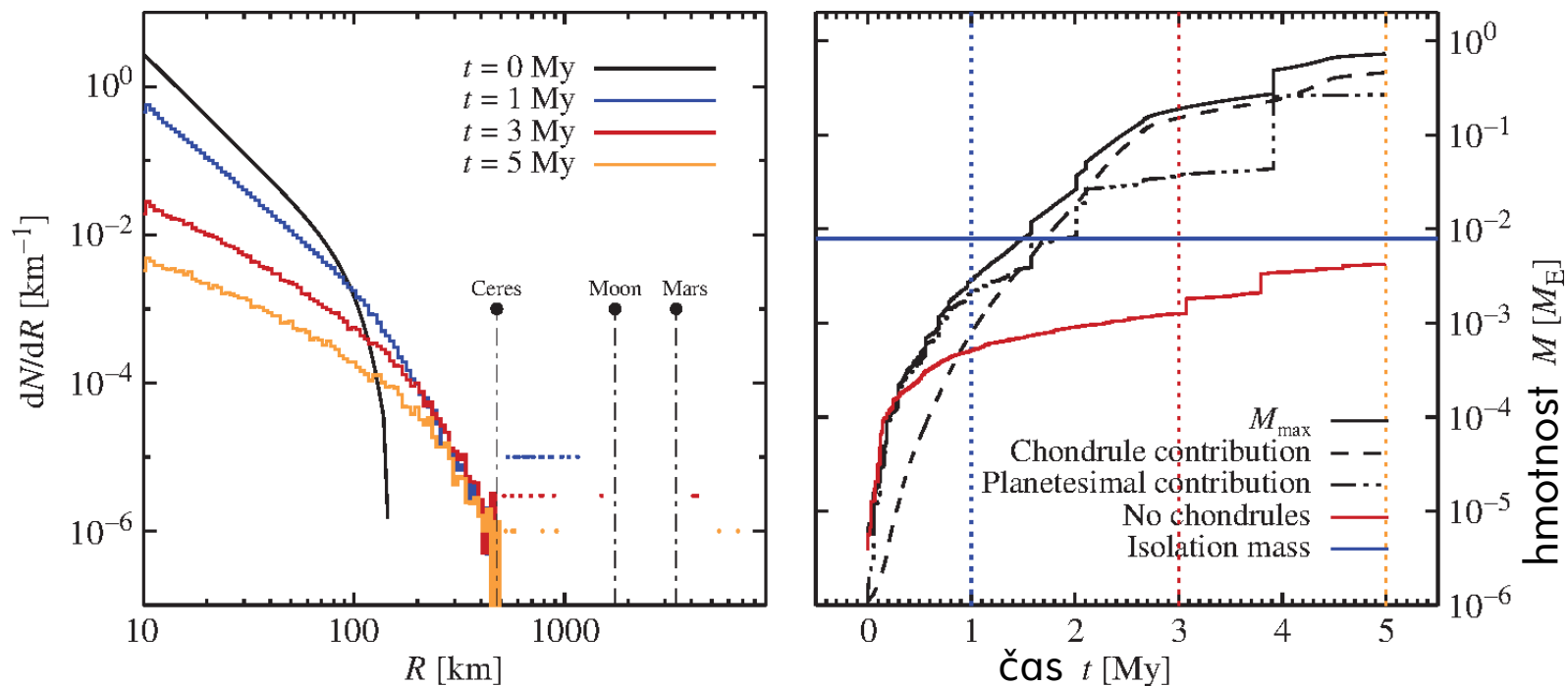
Lambrechts & Johansen (2012)

- drift & akrece balvanů
- aerodynamické tření blízko planety
- Bondiho vs Hillův režim
- a. na jádra obřích planet ($3 M_E$)



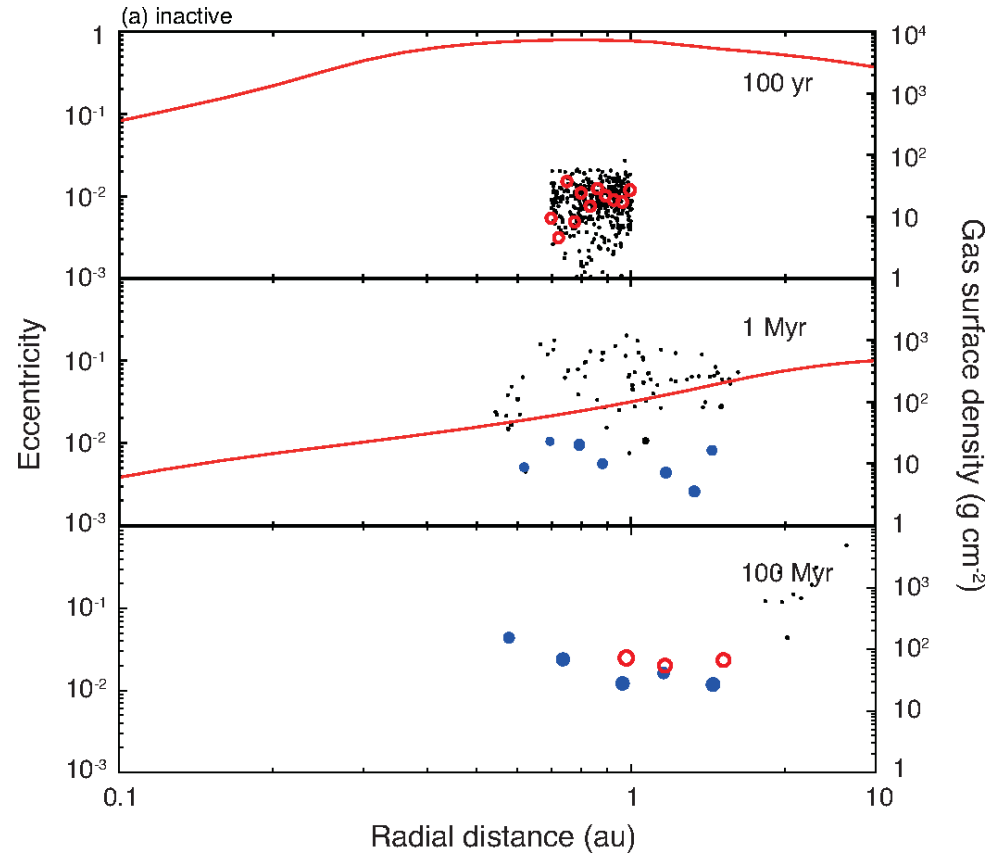
Johansen et al. (2015)

- rychlé formování Země (5 My) v plynném disku, s akrecí **chondrulí**



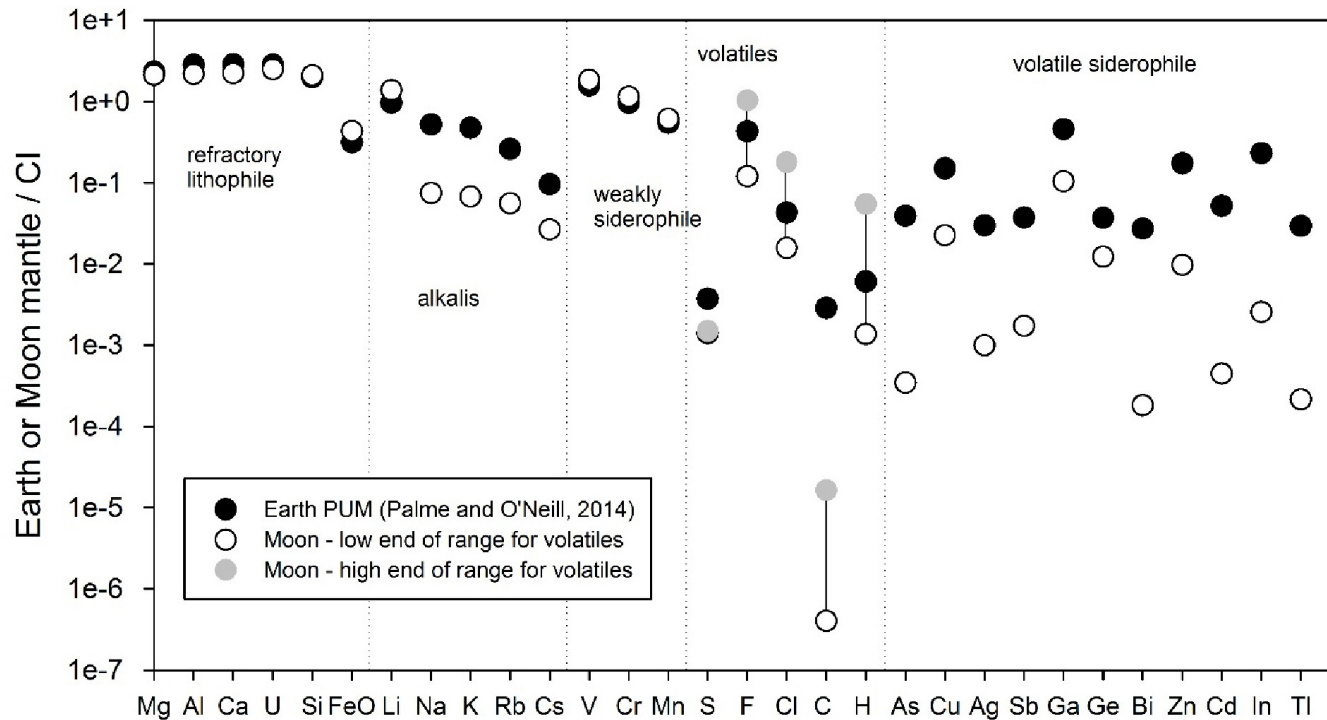
Ogihara et al. (2018)

- obrácený profil ξ & tření o plyn
→ soustředění **planetesimál**
- IC úzké mezikruží (jako Hansen)



Canup et al. (2019)

- Měsíc vs Země, resp. primitivní vrchní plášť (PUM), podobnost ch. složení!

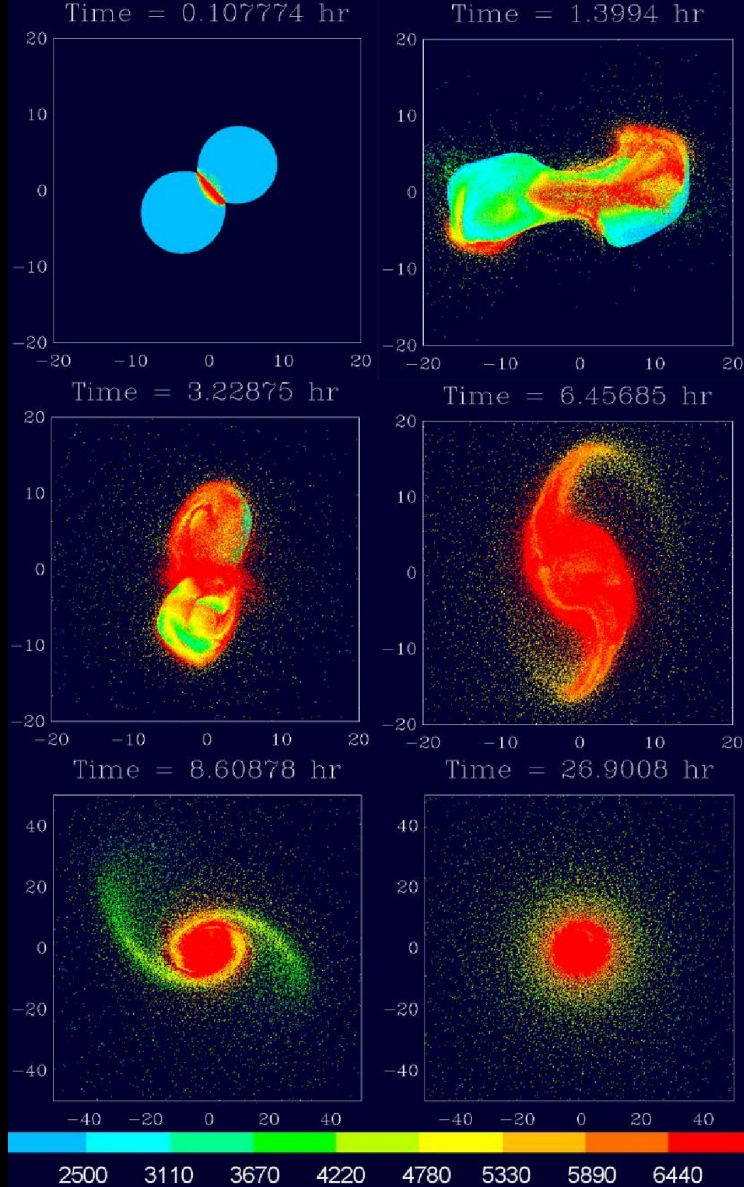


Canup (2012)

impakty 0.5/0.5 Země,
ale velké L ...

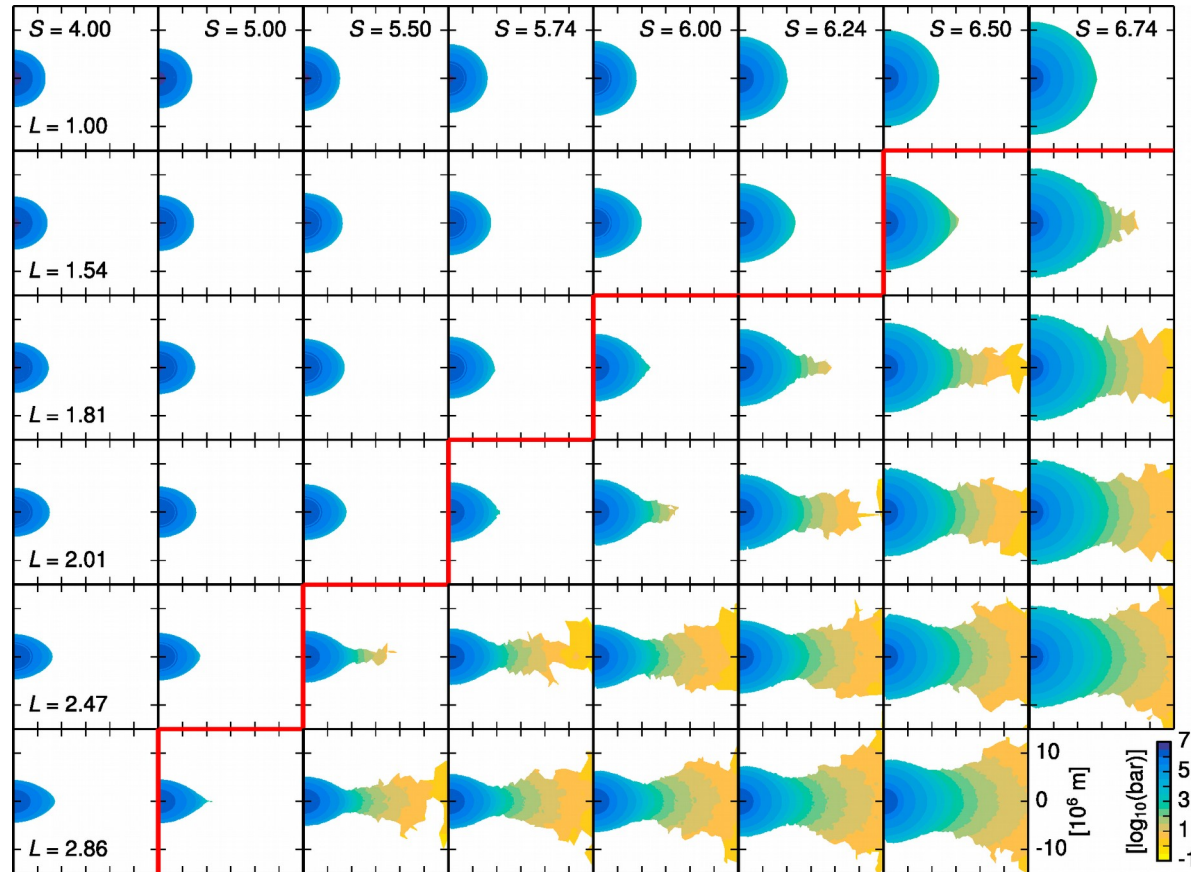
Cuk & Stewart (2012)

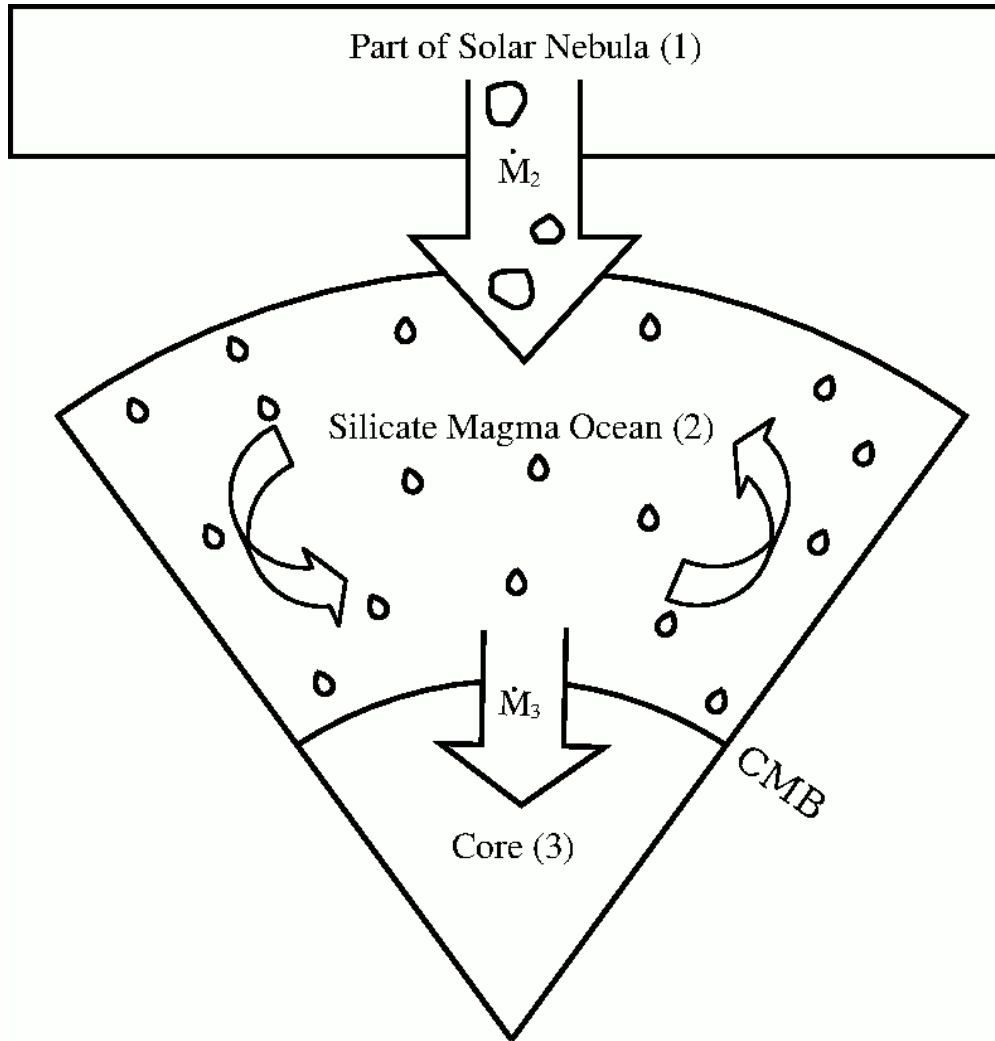
... evekční rezonance
→ přenos L



Lock & Stewart (2017)

- rychlá rotace nebo velký L_{imp}
- Země + disk = “synestia”





Geochemický model pozn. K. Walsh

wolfram hafnium siderofilní litofilní

rezervoáry: 1 .. mlhovina (CAI), 2 .. plášť, 3 .. jádro

veličiny: N počet atomů M hmotnost C koncentrace $\gamma \equiv \frac{M_3}{M}$ hmotnostní poměr

jádra $D \equiv \frac{C_3}{C_2}$ rozdělovací koeficient 1 rozhraní jádro/plášť (CMB)

1.1 Geochemické rovnice

transport stabilních izotopů zákon zachování wolframu Jacobsen (2009)

$$\dot{N}_1 + \dot{N}_2 + \dot{N}_3 = 0$$

$$\dot{N}_1 = -C_1 \dot{M} \quad (1)$$

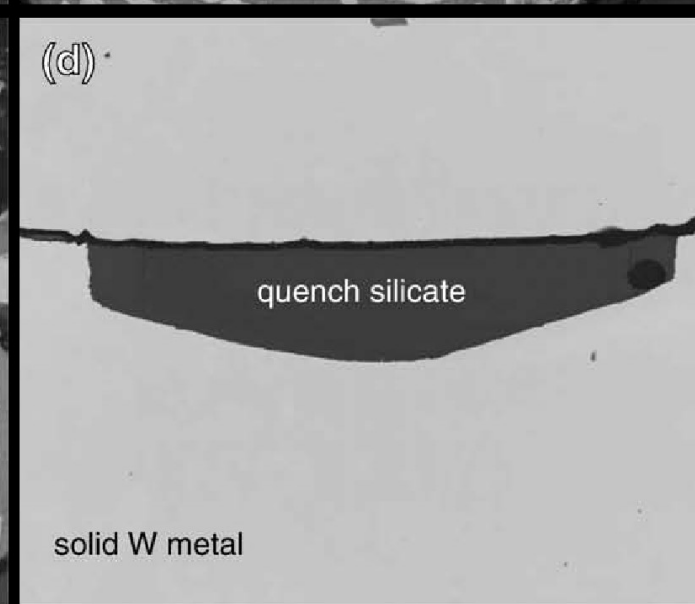
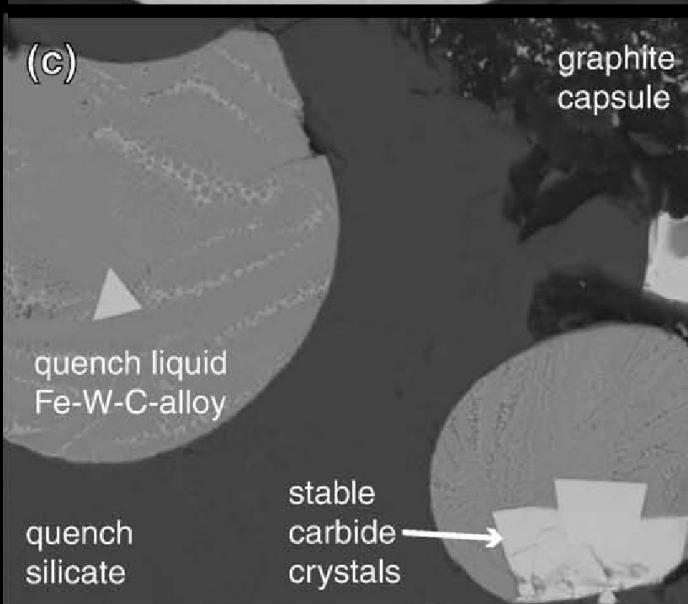
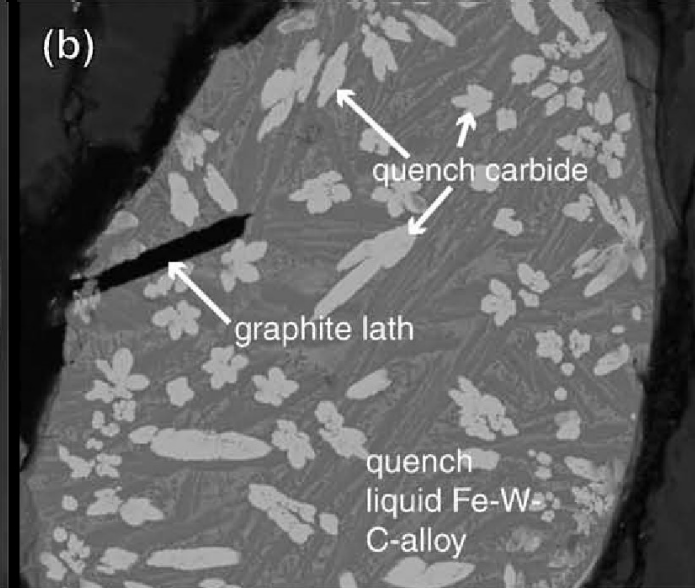
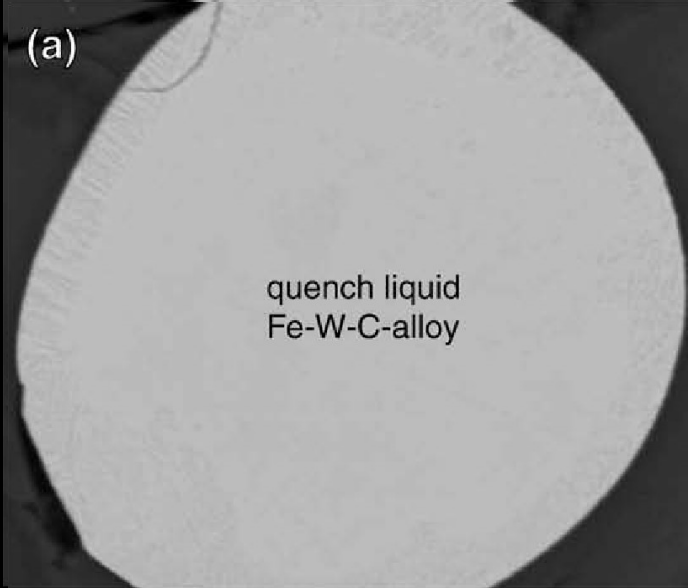
$$\dot{N}_2 = -\dot{N}_1 - \dot{N}_3 = C_1 \dot{M} - DC_2 \dot{M}_3 = (C_1 - \gamma DC_2) \dot{M} \quad (2)$$

$$\dot{N}_3 = \gamma DC_2 \dot{M} \quad (3)$$

koncentrace

$$C_2 = \frac{N_2}{M_2}$$

$$\dot{C}_2 = \dot{N}_2 \frac{1}{M_2} - N_2 \frac{1}{M_2^2} \dot{M}_2 = \frac{C_1 - (\gamma D + 1 - \gamma) C_2}{(1 - \gamma) M} \dot{M}$$



Geochemický model (2)

frakcionace Hf/W

$$f_2 \equiv \frac{N_{\text{Hf},2}/N_{\text{W},2}}{N_{\text{Hf},1}/N_{\text{W},1}} - 1 = \frac{N_{\text{W},1}}{N_{\text{W},2}} - 1 = \frac{N_{\text{W},1} - N_{\text{W},2}}{N_{\text{W},2}} = \frac{N_{\text{W},3}}{N_{\text{W},2}} \left(= \frac{N_3}{N_2} \right)$$

neboť Hf je silně litofilní ($N_{\text{Hf},3} \doteq 0$) stabilní izotopy ^{180}Hf , ^{183}W

$$\dot{f}_2 = \frac{\dot{N}_3}{N_2} - N_3 \frac{1}{N_2^2} \dot{N}_2,$$

dle (2), (3):

$$\dot{f}_2 = \gamma D C_2 \dot{M} \frac{1}{C_2 M_2} - \frac{N_3}{N_2} \frac{1}{C_2 M_2} (C_1 - \gamma D C_2) \dot{M} = \frac{\gamma D - f_2 \left(\frac{C_1}{C_2} - \gamma D \right)}{(1 - \gamma) M} \dot{M}$$

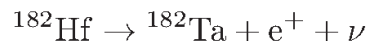
¹ je-li $D(t)$ a $\dot{M} > 0$, neplatí to neustále, ale jen pro \dot{M}

Geochemický model (3)

radiogenní izotop ^{182}W odchylka od mlhoviny (tzv. chondritického uniformního rezervoáru; CHUR)

$$\varepsilon_2 \equiv 10^4 \left(\frac{N_{182\text{W},2}/N_{183\text{W},2}}{N_{182\text{W},1}/N_{183\text{W},1}} - 1 \right)$$

radioaktivní rozpady (s poločasy $T_{1/2} = 9 \text{ Myr}$ a 144 d):



rozpadový zákon

$$\dot{N}_{182\text{Hf}} = -\lambda N_{182\text{Hf}}$$

$$\dot{N}_{182\text{W}} = +\lambda N_{182\text{Hf}}$$

$$N_{182\text{Hf}} = N_{182\text{Hf}}(0) e^{-\lambda t}$$

$$N_{182\text{W}} = N_{182\text{W}}(0) + N_{182\text{Hf}}(0)(1 - e^{-\lambda t}) \doteq N_{182\text{W}}(0)$$

jen několik ppm pak lze odvodit (Jacobsen 2005):

$$\dot{\varepsilon}_2 = Q^* f_2 - \frac{C_1}{C_2(1-\gamma)M} \dot{M} \varepsilon_2$$

$$Q^* = 10^4 \lambda e^{-\lambda t} \frac{C_{182\text{Hf},1}(0)}{C_{180\text{Hf},1}(0)} \frac{C_{180\text{Hf},1}(0)}{C_{182\text{W},1}(t)}$$

$C_{182\text{W},1}(t) \doteq C_{182\text{W},1}(0)$; liší se jen o několik ε

Geochemický model (4)

$$\dot{N}_{182W,2} = +\lambda N_{182Hf,2} + (C_1 - \gamma DC_2)\dot{M},$$

$$\dot{N}_{182W,1} = +\lambda N_{182Hf,1} - C_1\dot{M},$$

$$\dot{N}_{183W,1} = -C_1\dot{M},$$

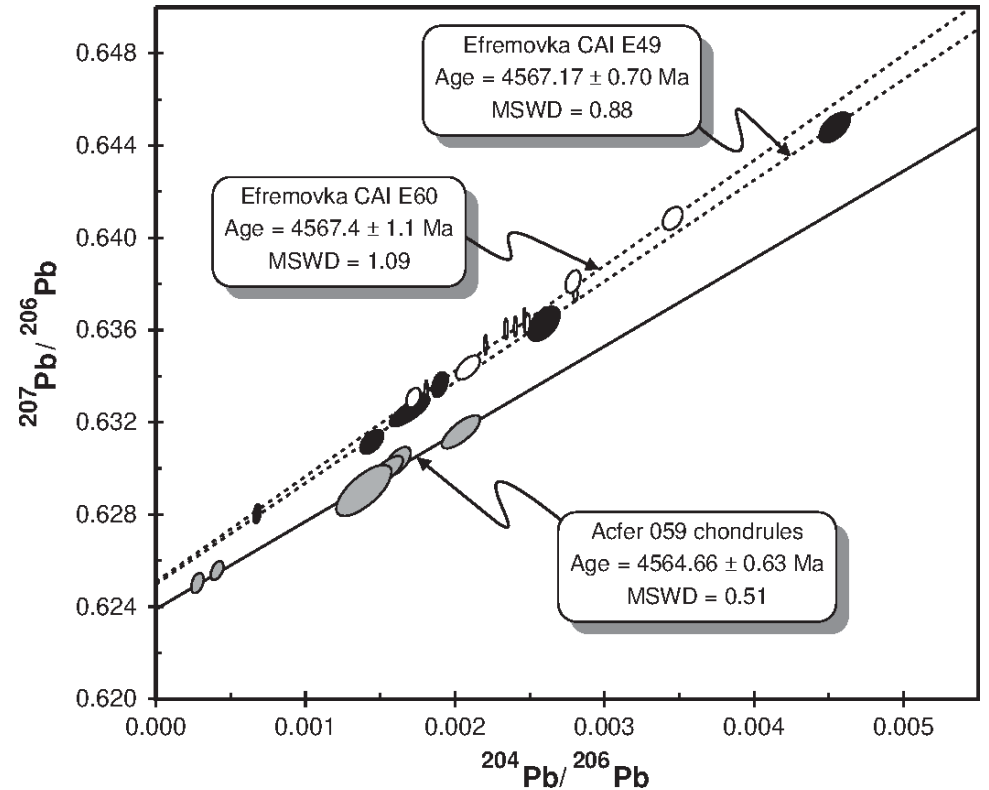
$$\dot{N}_{183W,2} = (C_1 - \gamma DC_2)\dot{M},$$

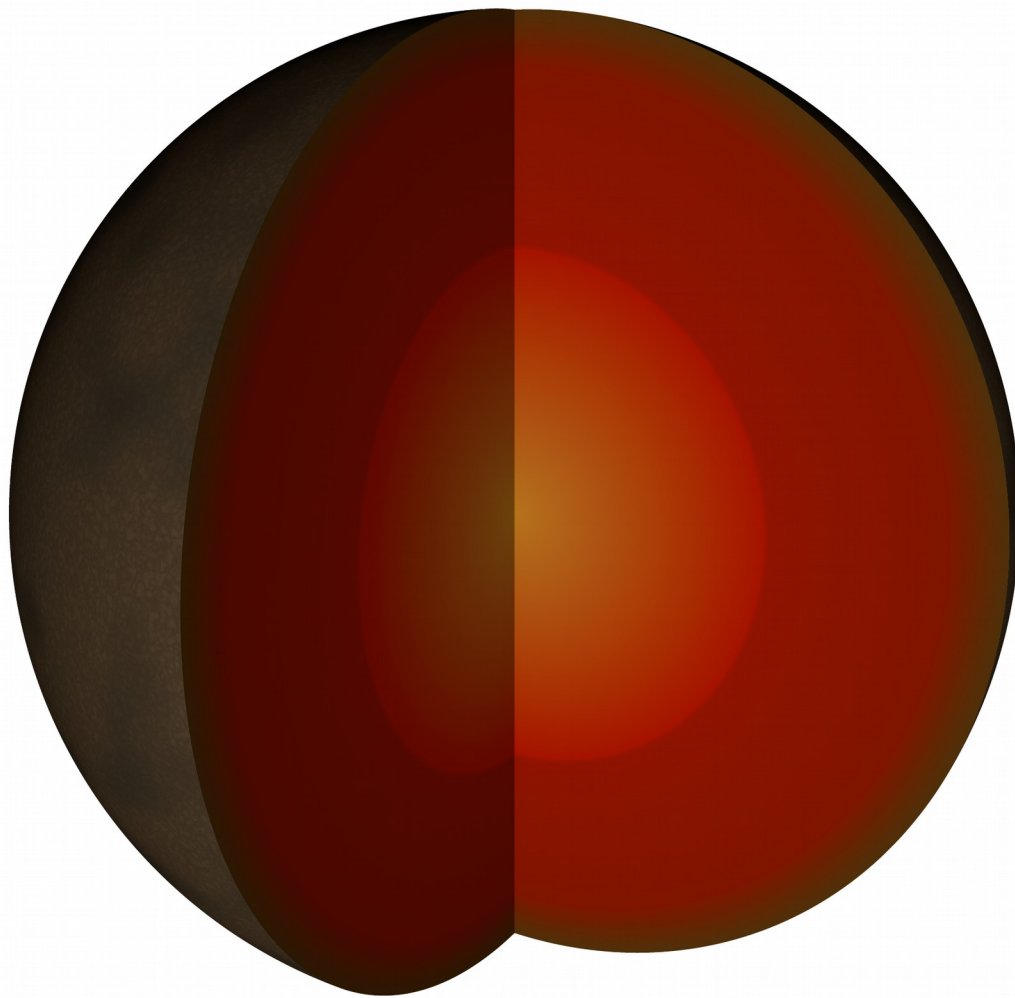
$$\begin{aligned} \dot{\varepsilon}_2 &= 10^4 \overbrace{\frac{N_{182W,2}}{N_{182W,1}} \frac{N_{183W,1}}{N_{183W,2}}}^{\doteq 1} \left(\frac{\dot{N}_{182W,2}}{N_{182W,2}} - \frac{\dot{N}_{182W,1}}{N_{182W,1}} + \frac{\dot{N}_{183W,1}}{N_{183W,1}} - \frac{\dot{N}_{183W,2}}{N_{183W,2}} \right) = \\ &= \dots \left(\lambda \frac{N_{182Hf,2}}{N_{182W,2}} + \frac{C_{182W,1}\dot{M}}{N_{182W,2}} - \frac{\gamma DC_{182W,2}\dot{M}}{N_{182W,2}} - \lambda \frac{N_{182W,1}}{N_{182W,1}} + \frac{C_{182W,1}\dot{M}}{N_{182W,1}} \right. \\ &\quad \left. - \frac{C_{183W,1}\dot{M}}{N_{183W,1}} - \frac{C_{183W,1}\dot{M}}{N_{183W,2}} + \frac{\gamma DC_{183W,2}\dot{M}}{N_{183W,2}} \right) = \\ &= \dots \lambda \left(\frac{N_{182Hf,2}}{N_{182W,2}} - \frac{N_{182W,1}}{N_{182W,1}} \right) + \dots \dot{M} \left(\frac{C_{182W,1}}{N_{182W,2}} - \frac{C_{183W,1}}{N_{183W,2}} \right) = \\ &= 10^4 \lambda \frac{C_{182Hf,1}(0)}{C_{182W,1}(t)} \frac{e^{-\lambda t}}{C_{180Hf,1}} \left(\frac{N_{182Hf,2}}{N_{182W,2}} \frac{N_{182W,1}}{N_{182Hf,1}} - 1 \right) + \\ &\quad + 10^4 \frac{C_{183W,1}}{C_{183W,2}} \frac{1}{(1-\gamma)M} \dot{M} \left(\frac{C_{182W,1}}{C_{182W,2}} \frac{C_{183W,2}}{C_{183W,1}} - 1 \right) = \\ &= Q^* f_2 + \frac{C_1}{C_2(1-\gamma)M} \dot{M} \varepsilon_2 \quad \text{c. b. d.} \end{aligned}$$

Kolik je 0?

- **CAI** (vápnito-hlinité inkluze)
- formování, resp. uzavření systému:
 $4,567 \pm 0,001$ Gy

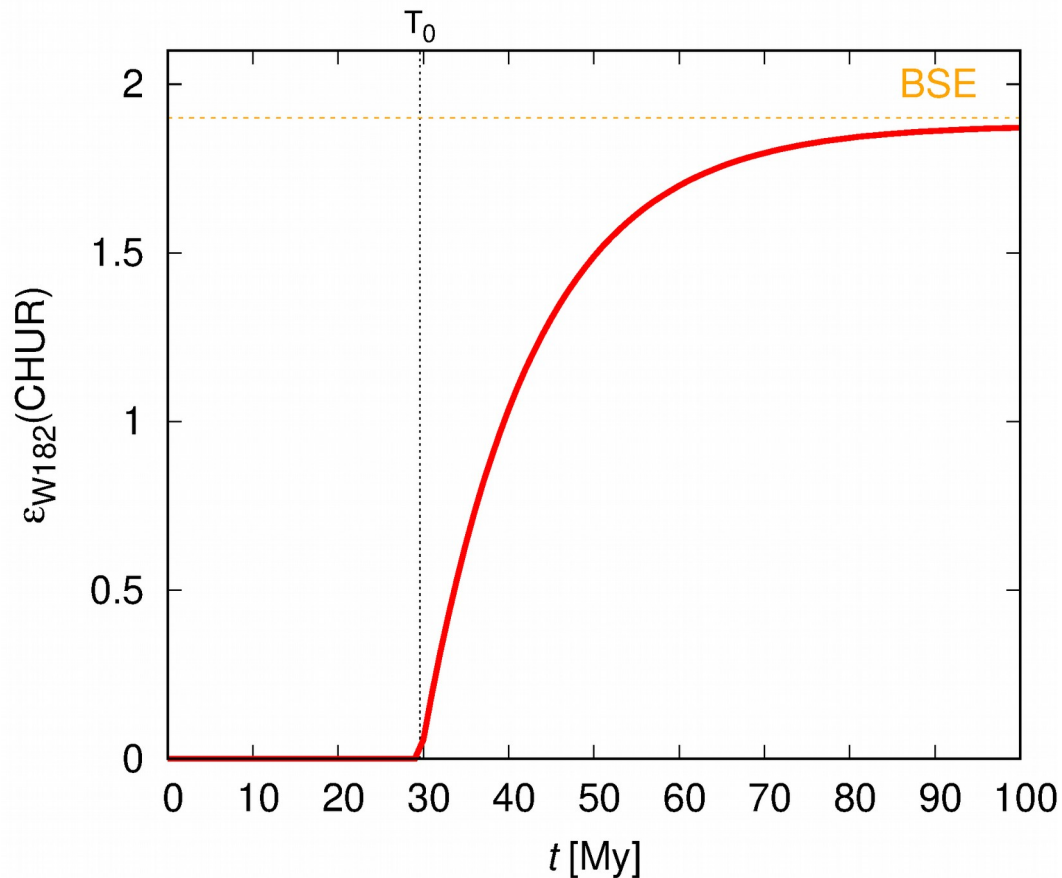
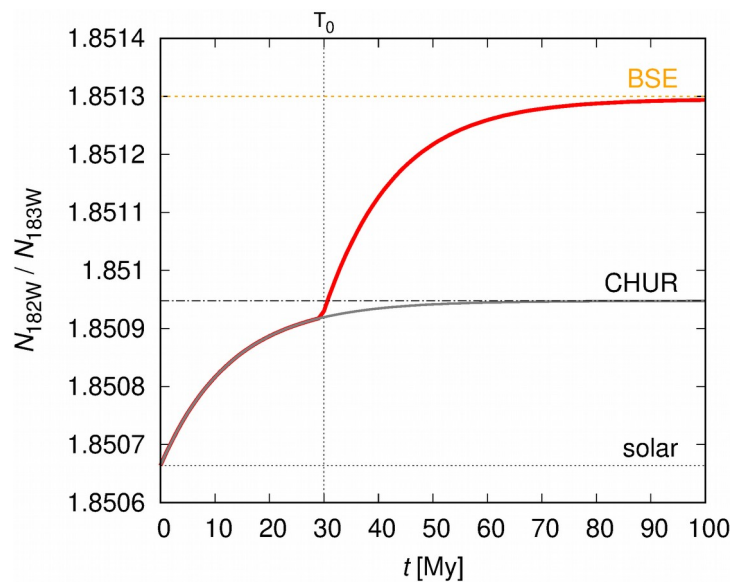
(Amelin et al. 2002)





Diferenciace Země

- nejjednodušší g. m.: 1 událost
- měřené $\epsilon_{182\text{W}}$ (CHUR) = 1.9 ± 0.1
→ 30 My (po CAI)

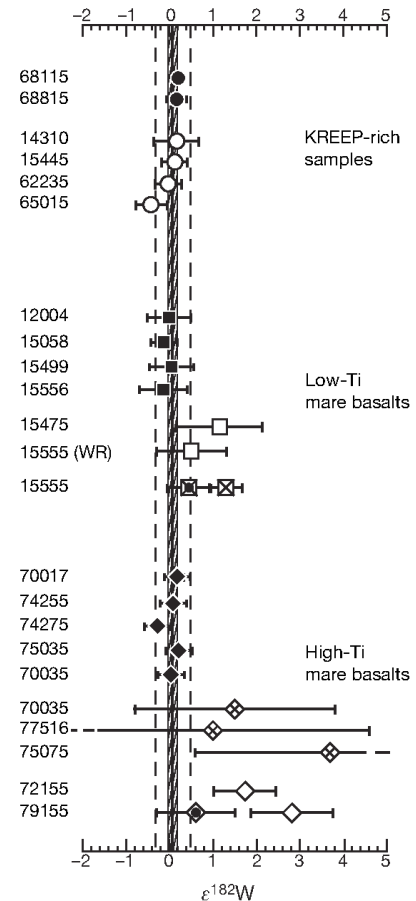


Touboul et al. (2007)

↓ minerály bez Ta

- systém Hf/W, opr. o kosmogenický $^{181}\text{Ta} \rightarrow ^{182}\text{W}$
- $\epsilon_{182\text{W}}$ (BSE) = 0.09 ± 0.10
- diferenciace Měsíce $> 62_{-10}^{+90}$ My (po CAI)

BSE ... silikátový plášť+kůra Země



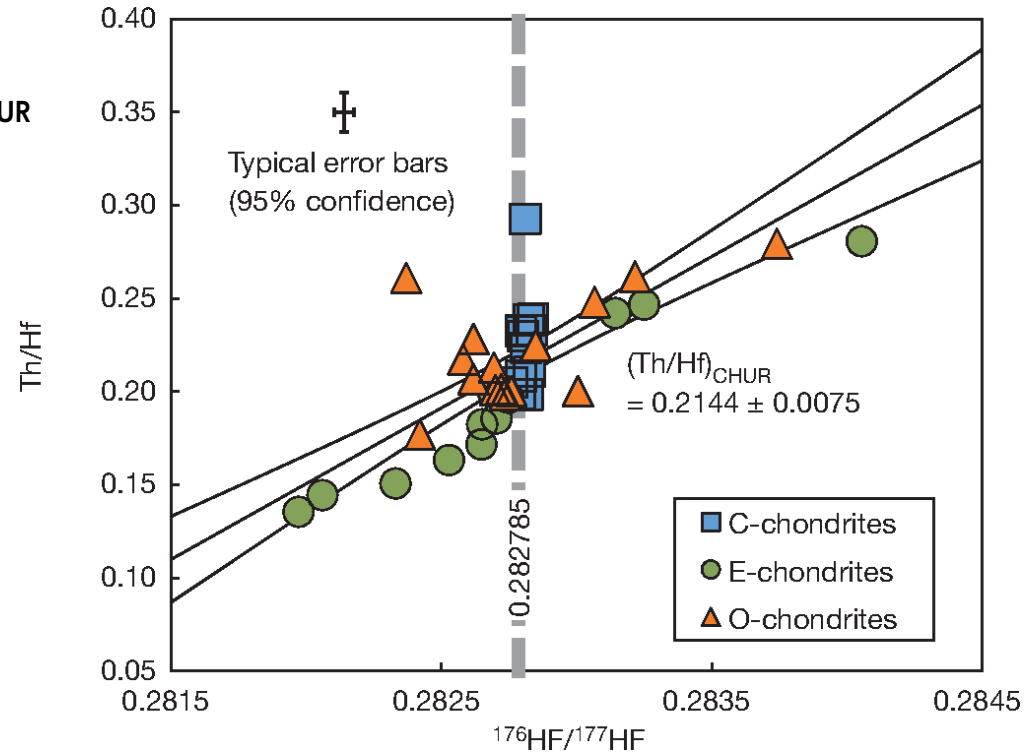
Dauphas & Pourmand (2011)

↓ měřící rce.

- $Hf/W = (Th/W) / (Th/Hf)$
- $(Hf/W)_{\text{plášť Marsu}} \doteq (Th/W)_{\text{SNC}} / (Th/Hf)_{\text{CHUR}}$
- $Hf/W = 3.51 \pm 0.45$
- $t_{1/2} = 1.8_{-1.0}^{+0.9} \text{ My}$, tzn. **mladý Mars!**

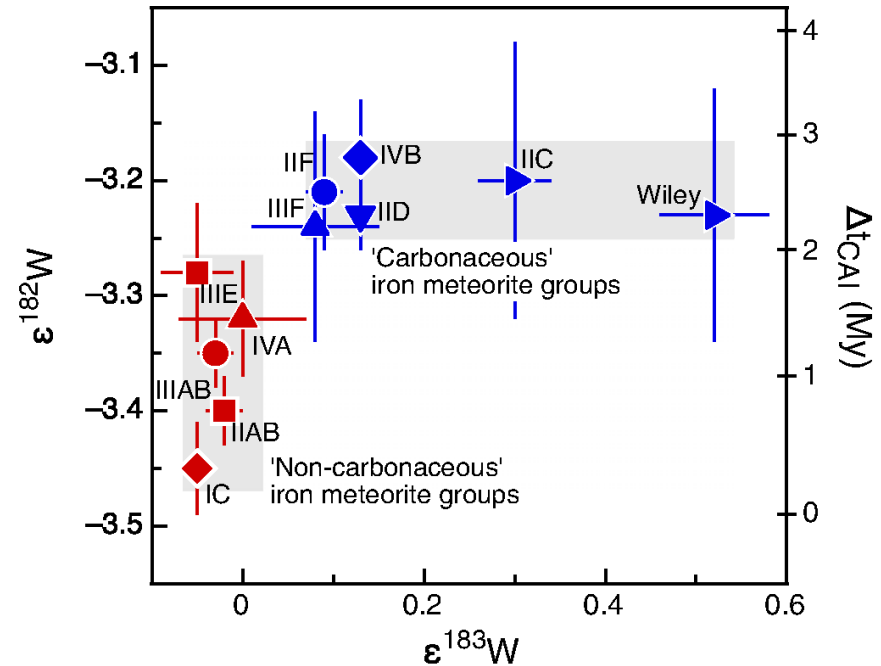
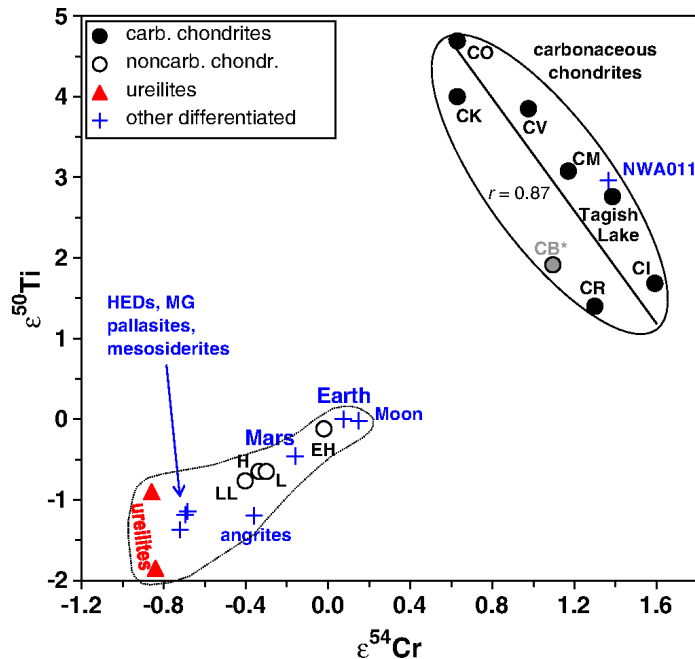
SNC ... marsovské meteority (shergottity, ...)

CHUR ... chondritický uniformní rezervoár



Warren (2011), Kruijer et al. (2017)

- dichotomie izotopů: $^{50}\text{Ti}/^{54}\text{Cr}$, $^{17}\text{O}/^{54}\text{Cr}$, $^{54}\text{Cr}/^{65}\text{Ni}$, $^{95}\text{Mo}/^{94}\text{Mo}$, $^{182}\text{W}/^{183}\text{W}$, ...
- oddělení rezervoárů **CC** (uhlíkatý ch.) & **NC** (ne...) ← Jupiterova mezera?!



Kruijer et al. (2017)

CAI (vápnito-hlinité inkluze)
čas formování (4.567 ± 0.001) Gy
(Amelin et al. 2002)

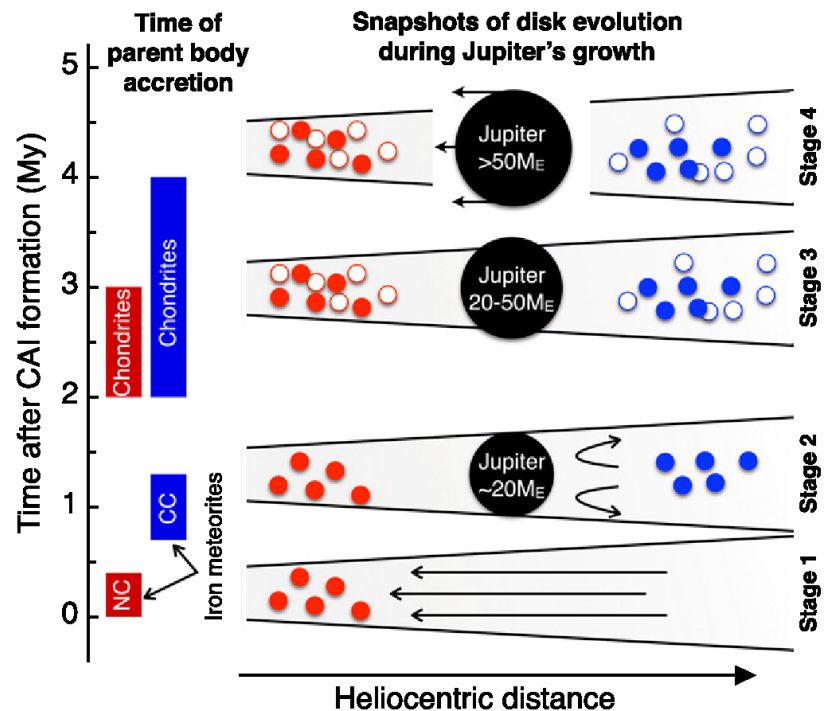


Fig. 4. Four snapshots of Jupiter's growth in the solar circumstellar disk. At stage 1, within <0.4 My after CAI, the NC iron meteorite parent bodies (red solid symbols) accreted in a continuous gas disk characterized by inward drag of solids. At stage 2, around ~ 1 My after CAI, iron meteorite parent bodies of the CC reservoir (blue solid symbols) had accreted and Jupiter had already grown to $\sim 20 M_E$, preventing any inward drag of solids (24). At stage 3, from ~ 2 My to ~ 4 My after CAI, Jupiter grew further through gas accretion onto its core. Moreover, the ordinary chondrite parent bodies (red open symbols) accreted in the NC reservoir and CC chondrite parent bodies (blue open symbols) in the CC reservoir. At stage 4, after ~ 3 – 4 My after CAI, Jupiter had grown to $\sim 50 M_E$ and had opened a gap in the disk (13, 23, 24), likely resulting in the inward migration of Jupiter. Solid boxes (*Left*) show the accretion ages of iron meteorite and chondrite parent bodies in the NC and CC reservoirs (see *CC and NC Iron Meteorites*).

Burkhardt et al. (2019)

“CC = NC + IC”

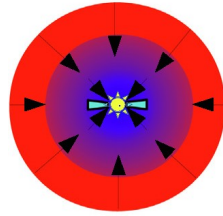
CC ... uhlíkatý chondritický

NC ... neuhlíkatý ch.

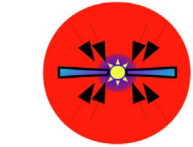
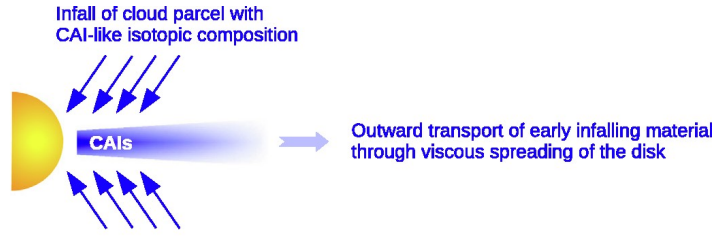
IC ... jako inkluze, chemicky ch.,
isotopicky CAI

heterogenenní akrece!

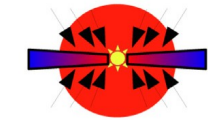
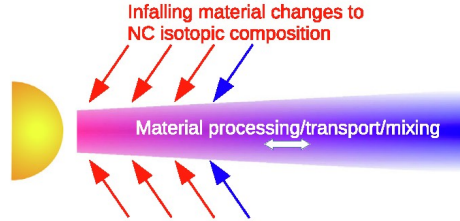
teplotní přepracování nikoliv,
změnilo by ch. složení



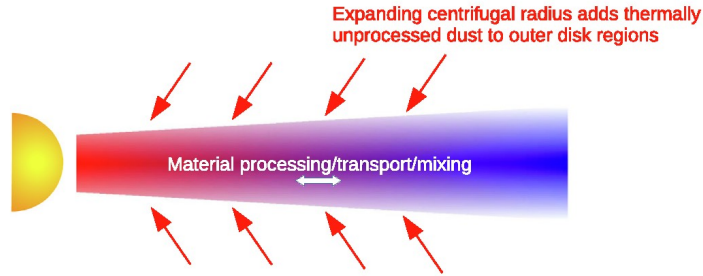
A



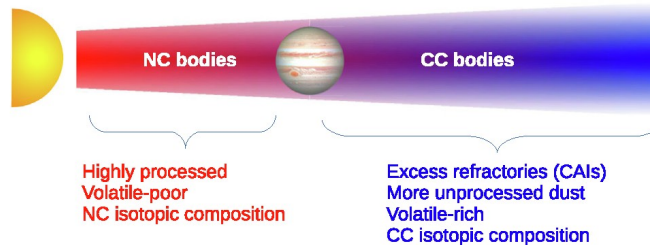
B



C



D



Lammer et al. (2018)

- výpařování nebo únik atmosféry → spíše lehké izotopy → snížení $^{20}\text{Ne}/^{22}\text{Ne}$, $^{36}\text{Ar}/^{38}\text{Ar}$ (z počátečních CAI) → hmotnost a. → hmotnost planety (v plynu)

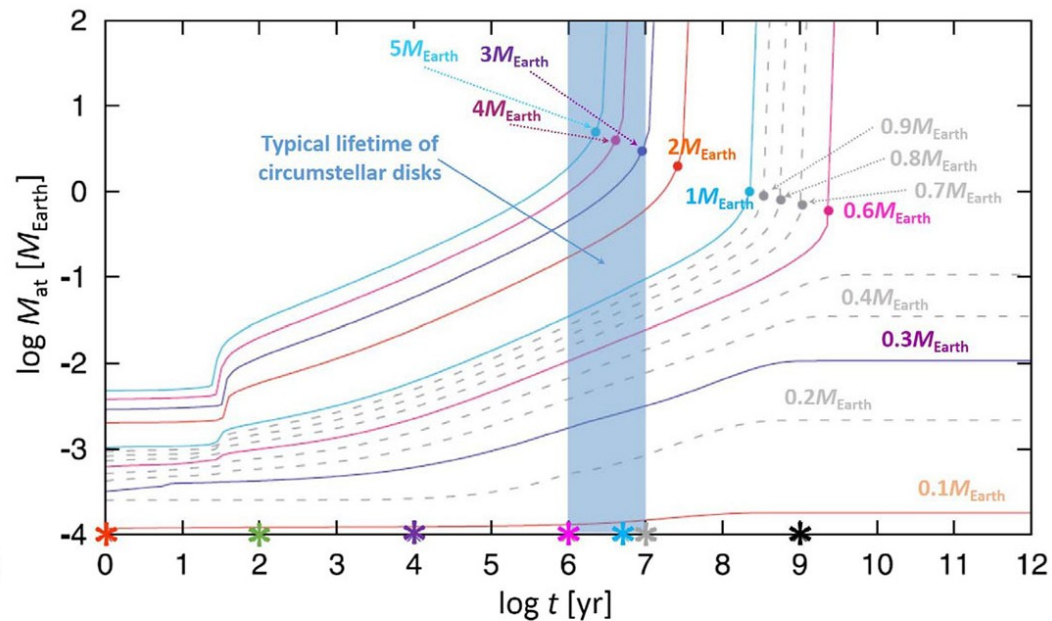
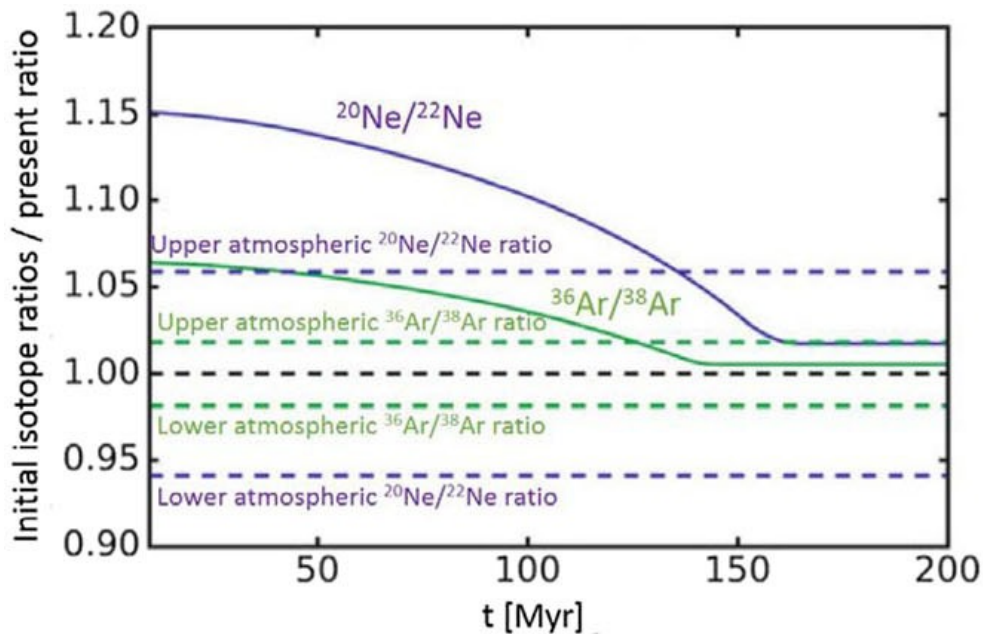
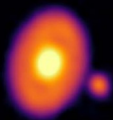


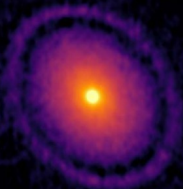
Fig. 2. Total mass of accumulated H_2 envelopes within the Hill sphere as a function of time

HT Lup

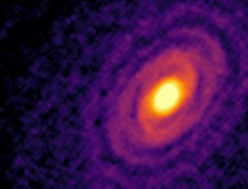


10 au

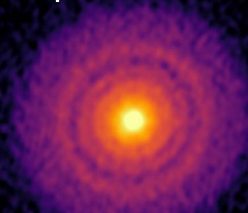
GW Lup



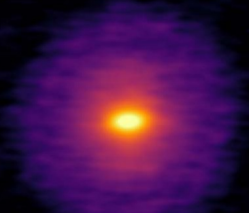
IM Lup



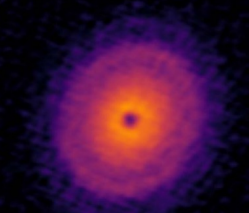
RU Lup



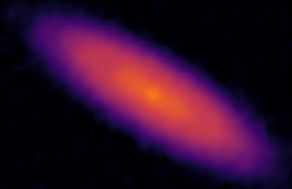
Sz 114



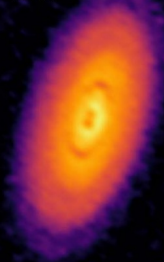
Sz 129



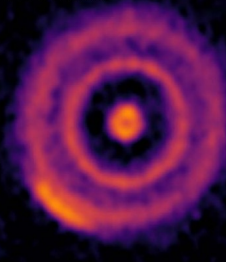
MY Lup



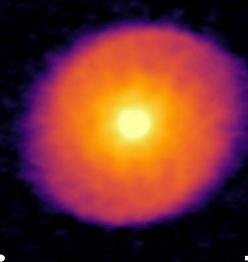
HD 142666



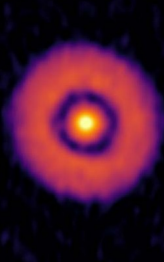
HD 143006



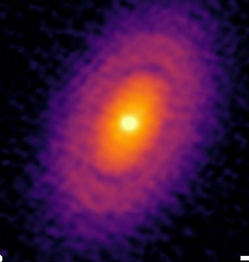
AS 205



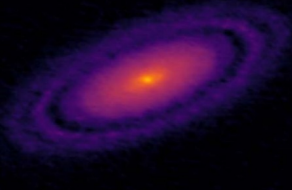
SR 4



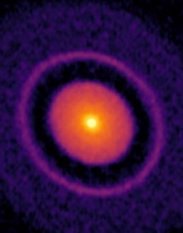
Elias 20



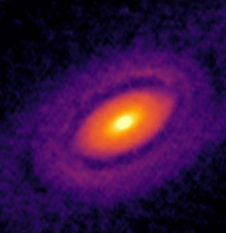
DoAr 25



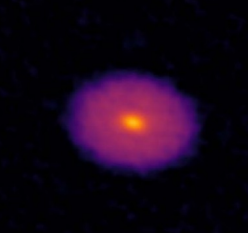
Elias 24



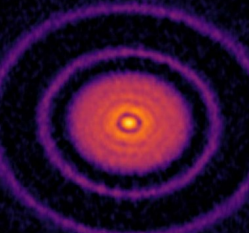
Elias 27



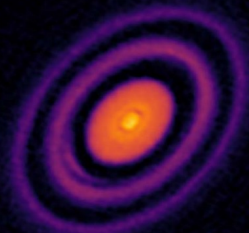
DoAr 33



AS 209



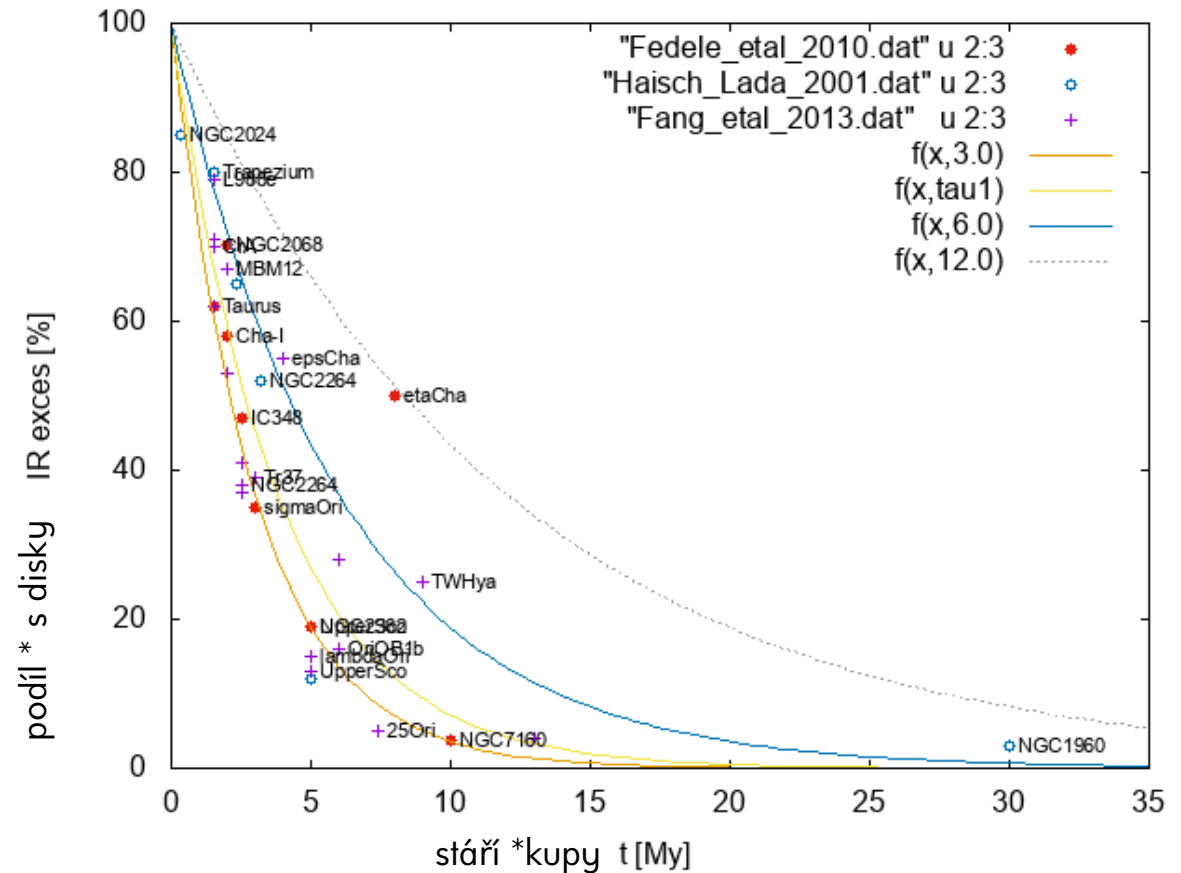
HD 163296



Andrews et al. (2018); viz velikost svazku; prach & plyn (VLT/SPHERE) ~ podobné struktury → planety!

Fedele et al. (2010)

- podíl * s diský (přebytek IR)
- stáří * kupy → stáří disku?
- existují staré! (TW Hya, η Cha)



Wetherill (1990), p. 30

Effects of Nebular Gas During the Final Stage of Accumulation

Annu. Rev. Earth Planet. Sci. 1
Access provided by Charles Unive.

part of the nebula on a time scale that is short (e.g. $\sim 10^5$ yr at 1 AU) compared with the time scale for removal of all of the nebular gas. Thus, gas-free final accumulation of the terrestrial planets might proceed before the giant planets had completed their growth.

Now, however, it seems likely that runaway embryos are likely to form quite rapidly, in $\sim 10^5$ yr, and this places more strain on this hypothesized chain of events. In addition, it has also been proposed (Takeda et al 1985) that for planetary embryos the gas drag coefficient may be greatly enhanced for a gravitating body at low values of the Reynolds number ($Re \sim 20$). Ohtsuki et al (1988) have pursued the consequences of this enhanced gas drag. They find, among other things, that gas drag could then be the dominant "damping" force during the coalescence of embryos; that gas-drag-induced radial migration of large embryos may be important, in addition to that caused by tidal density wave effects (Ward 1986); and that relative velocities during the final stage of accumulation may be significantly lower than in the more popular gas-free case. Provided that all these inadequately studied effects can actually produce a system of

překotně vznikající embrya
za 10^5 let

tření o plyn
tlumící síla
radiální migrace embryjí
slapy hustotních vln

FORMATION OF THE EARTH 235

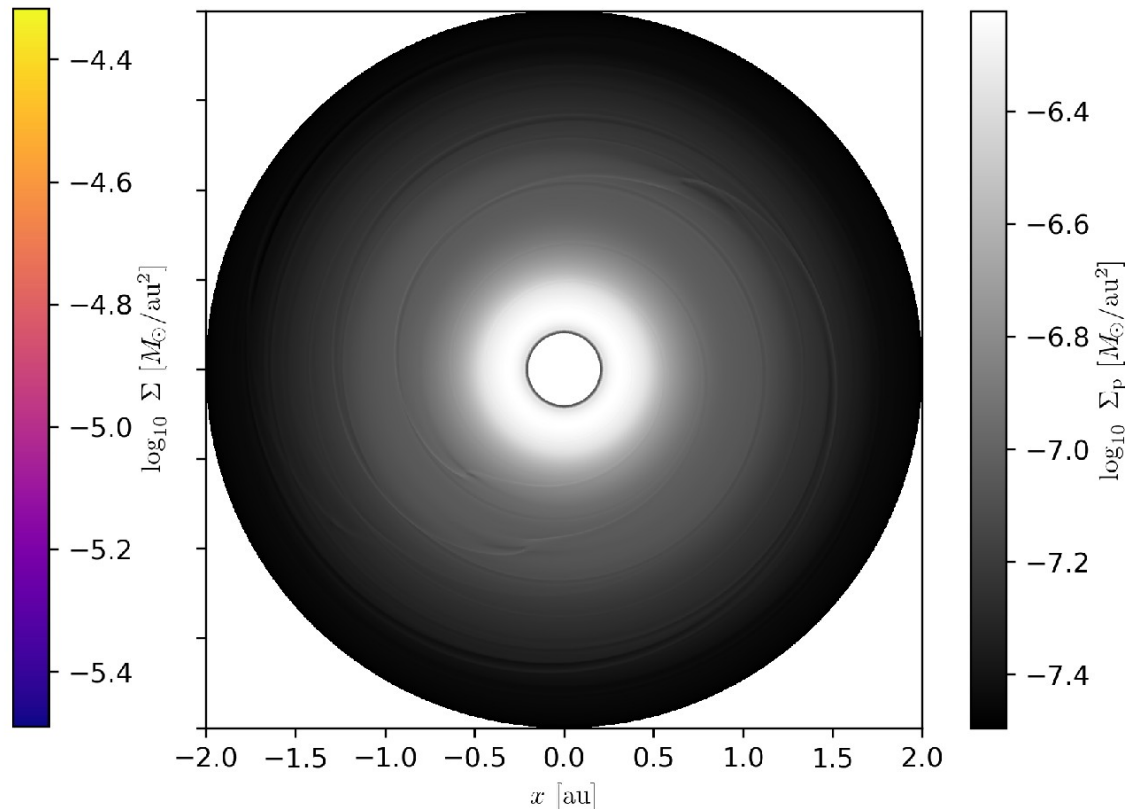
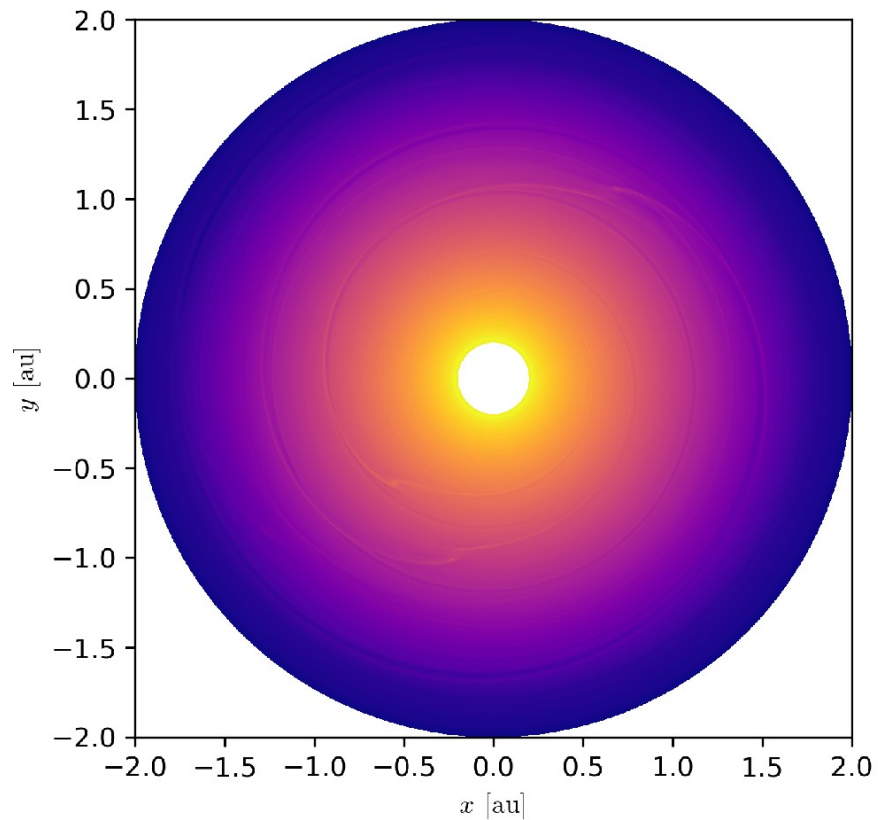
terrestrial planets similar to that observed, it is also quite likely that the time scale for the final growth of the Earth could be as short as 10^7 yr, which suggests that capture of a very massive ($> 10^{26}$ g) and very hot (~ 3000 K) primitive atmosphere (Hayashi et al 1979) might then be expected if the nebular gas were still present at 1 AU for as long as 10^7 yr.

Ohtsuki et al (1988) conclude that the effects described above may be overestimated because of oversimplifications in the theoretical treatment of Takeda et al (1985), e.g. the assumption of Reynolds numbers lower than those expected in the solar nebula and the neglect of solar gravity. Nevertheless, subject to much more quantitative scrutiny, an evolution of this kind may be considered to be an alternative to the more conventional gas-free final accumulation of the terrestrial planets. This alternative could have observationally distinguishable consequences, but these have not yet been worked out completely enough to be discussed in a responsible way at present.

růst Země za 10^7 let
primitivní atmosféra

www.annualreviews.org
17/19. For personal use only.

Radiační hydrodynamika (RHD)



plyn

$$\frac{\partial \Sigma}{\partial t} + \mathbf{v} \cdot \nabla \Sigma = -\Sigma \nabla \cdot \mathbf{v} - \left(\frac{\partial \Sigma}{\partial t} \right)_{\text{acc}}, \quad (1)$$

$$\frac{\partial \mathbf{v}}{\partial t} + \mathbf{v} \cdot \nabla \mathbf{v} = -\frac{1}{\Sigma} \nabla P + \frac{1}{\Sigma} \nabla \cdot \mathbb{T} - \frac{\int \rho \nabla \phi dz}{\Sigma} + \frac{\Sigma_p}{\Sigma} \frac{\Omega_K}{\tau} (\mathbf{u} - \mathbf{v}), \quad (2)$$

$$\begin{aligned} \frac{\partial E}{\partial t} + \mathbf{v} \cdot \nabla E = & -E \nabla \cdot \mathbf{v} - P \nabla \cdot \mathbf{v} + Q_{\text{visc}} + \frac{2\sigma T_{\text{irr}}^4}{\tau_{\text{eff}}} - \frac{2\sigma T^4}{\tau_{\text{eff}}} + \\ & + 2H \nabla \cdot \frac{16\sigma \lambda_{\text{lim}}}{\rho_0 \kappa_R} T^3 \nabla T + \sum_i \frac{GM_i \dot{M}_i}{R_i S_{\text{cell}}} \delta(\mathbf{r} - \mathbf{r}_i), \end{aligned} \quad (3)$$

$$P = \Sigma \frac{RT}{\mu} = (\gamma - 1)E, \quad (4)$$

Masset (2000)
Rein & Spiegel (2015)
Chrenko et al. (2017)



Warning
High
temperature

balvány

$$\frac{\partial \Sigma_p}{\partial t} + \mathbf{u} \cdot \nabla \Sigma_p = -\Sigma_p \nabla \cdot \mathbf{u} - \left(\frac{\partial \Sigma_p}{\partial t} \right)_{\text{acc}} - \left(\frac{\partial \Sigma_p}{\partial t} \right)_{\text{evap}}, \quad (5)$$

$$\frac{\partial \mathbf{u}}{\partial t} + \mathbf{u} \cdot \nabla \mathbf{u} = -\frac{\int \rho_p \nabla \phi dz}{\Sigma_p} - \frac{\Omega_K}{\tau} (\mathbf{u} - \mathbf{v}), \quad (6)$$

protoplanety

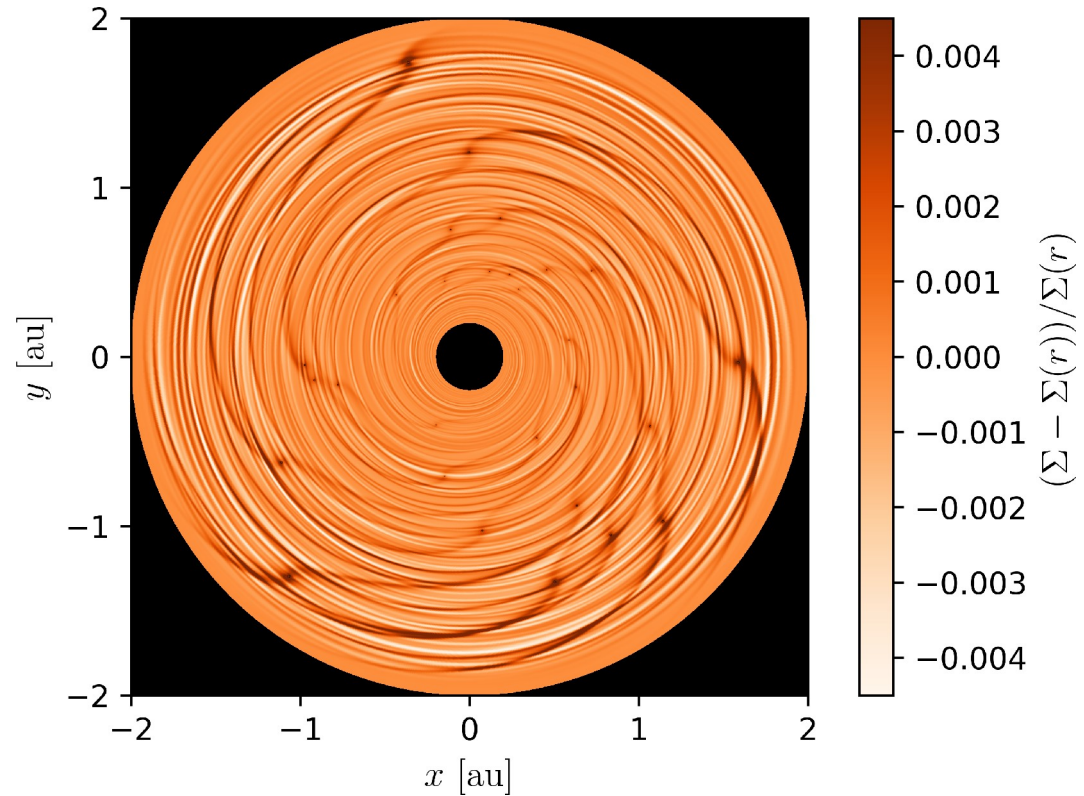
$$\dot{M}_i = \iint \left[\left(\frac{\partial \Sigma}{\partial t} \right)_{\text{acc}} + \left(\frac{\partial \Sigma_p}{\partial t} \right)_{\text{acc}} \right] r d\theta dr \quad \text{for } \forall i, \quad (7)$$

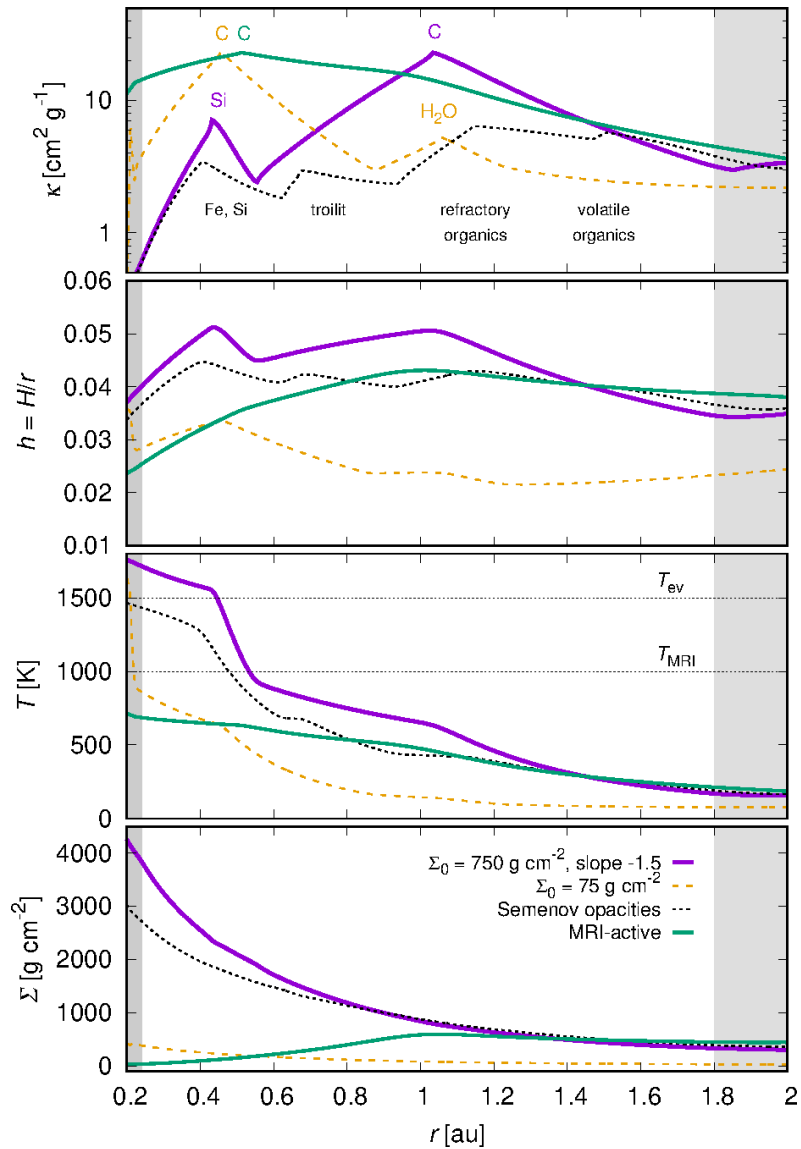
$$\begin{aligned} \ddot{\mathbf{r}}_i = & -\frac{GM_\star}{r_i^3} \mathbf{r}_i - \sum_{j \neq i} \frac{GM_j}{|\mathbf{r}_i - \mathbf{r}_j|^3} (\mathbf{r}_i - \mathbf{r}_j) + \iiint \frac{\rho \nabla \phi_i dz}{M_i} r d\theta dr + \\ & + f_z \hat{z} - \frac{1}{2} C \frac{\pi R_i^2}{M_i} \rho |\dot{\mathbf{r}}_i - \mathbf{v}_{\text{cell}}| (\dot{\mathbf{r}}_i - \mathbf{v}_{\text{cell}}) + \iint \left[\mathbf{v} \left(\frac{\partial \Sigma}{\partial t} \right)_{\text{acc}} + \mathbf{u} \left(\frac{\partial \Sigma_p}{\partial t} \right)_{\text{acc}} \right] r d\theta dr \end{aligned} \quad (8)$$

for $\forall i,$

Terestrické planety v disku

- Brož, Chrenko, Nesvorný, Dauphas (submit.)

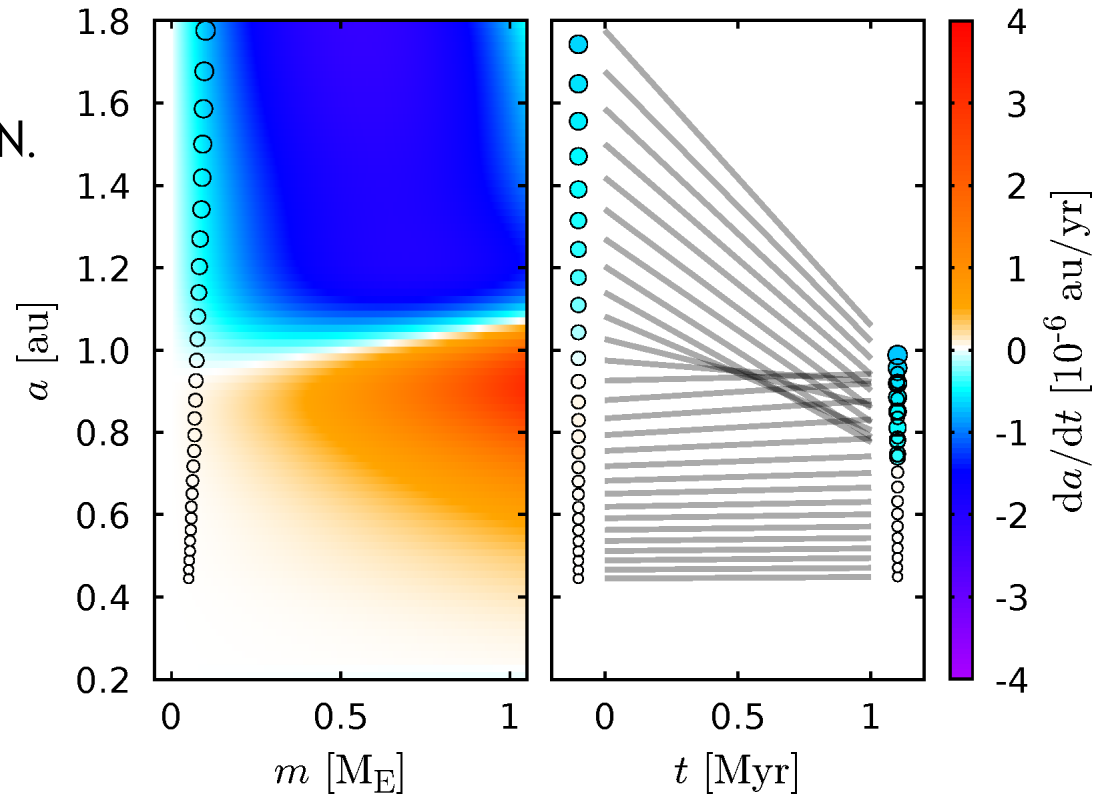




počáteční podmínky (IC):
 Kretke & Lin (2012)
 Ogihara et al. (2018)

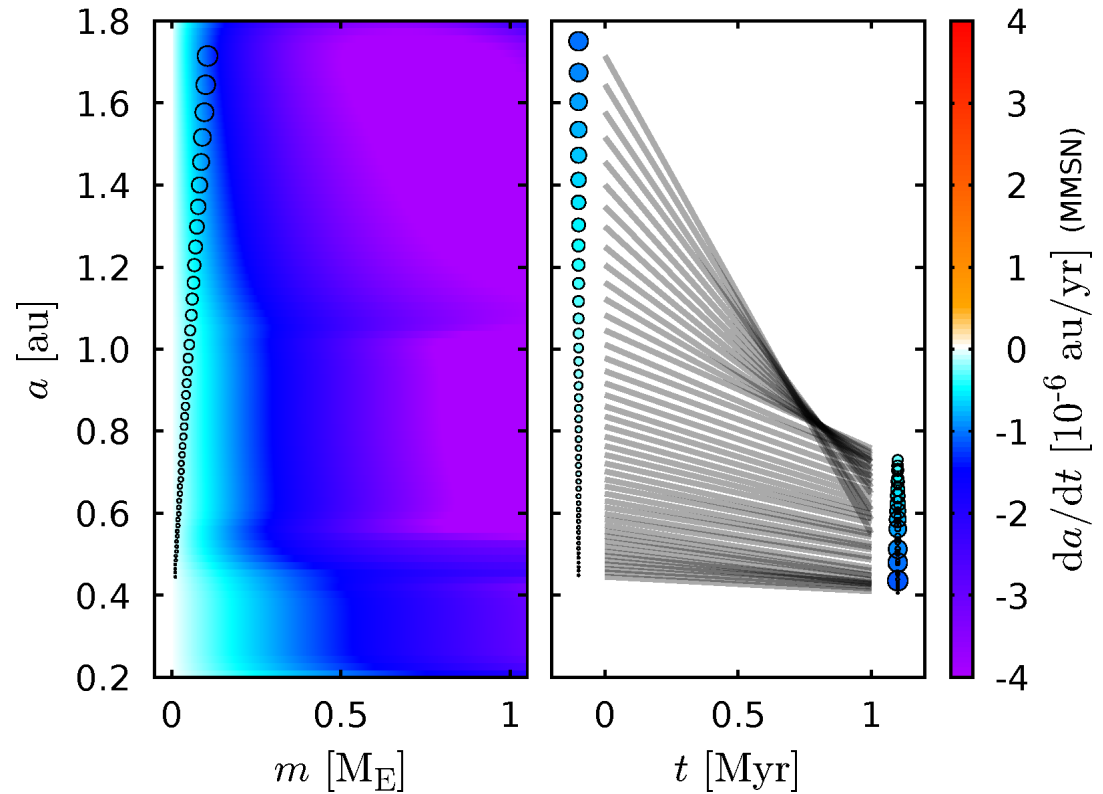
Konvergence drah

- MMSN neplatí!
- konvergence **před** rozplynutím N.

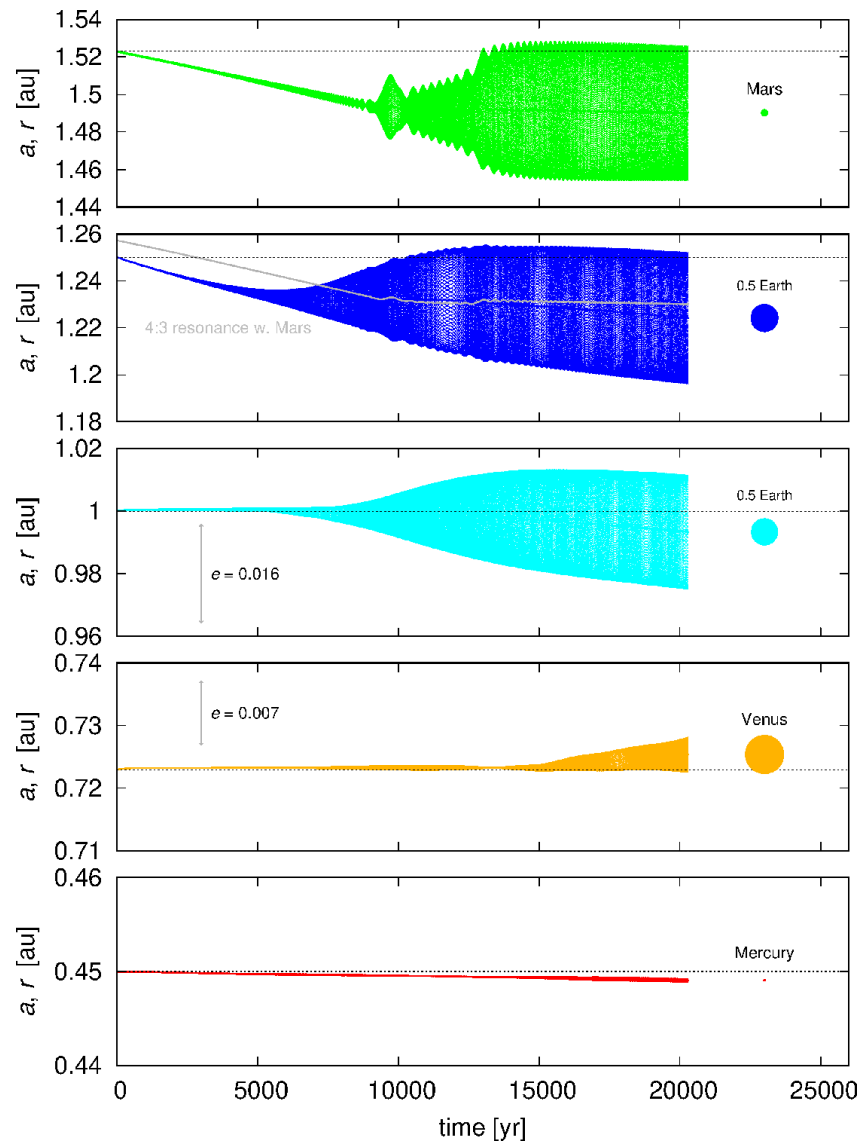


Konvergenz v MMSN

- $\sigma_{\text{MMSN}} = 1700 \text{ g/cm}^2 (r/1 \text{ au})^{-3/2}$

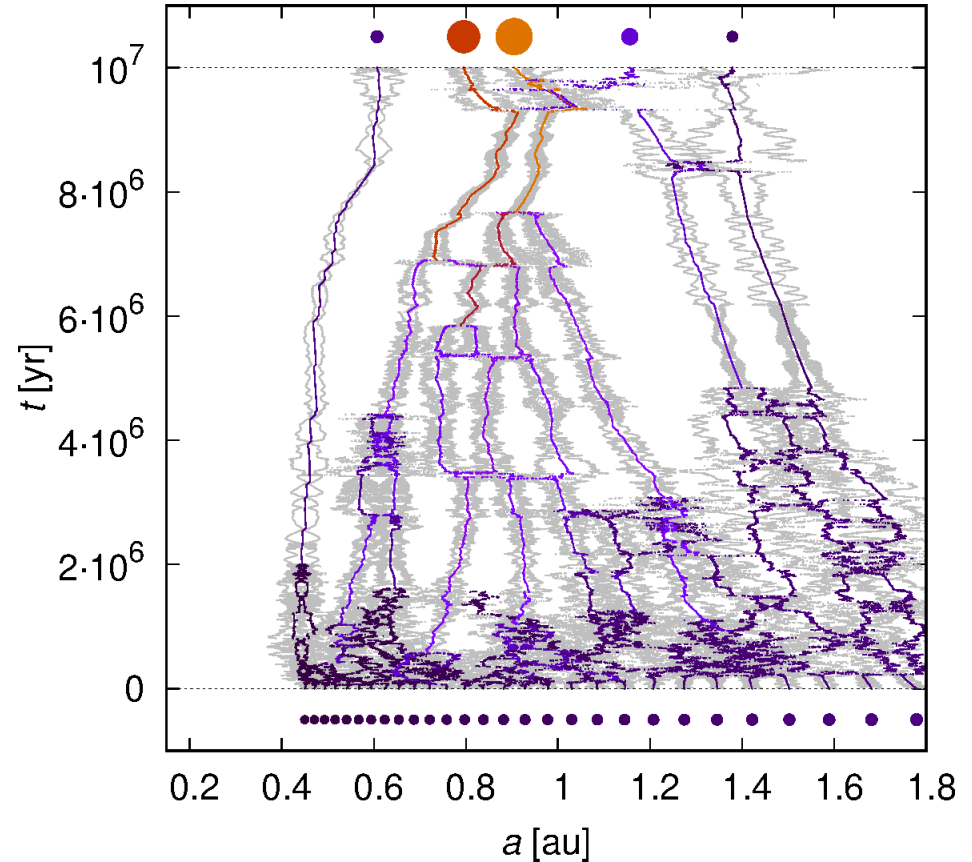


horká stopa → zvýšení e
až na současnou hodnotu
pro Venuši a Zemi!



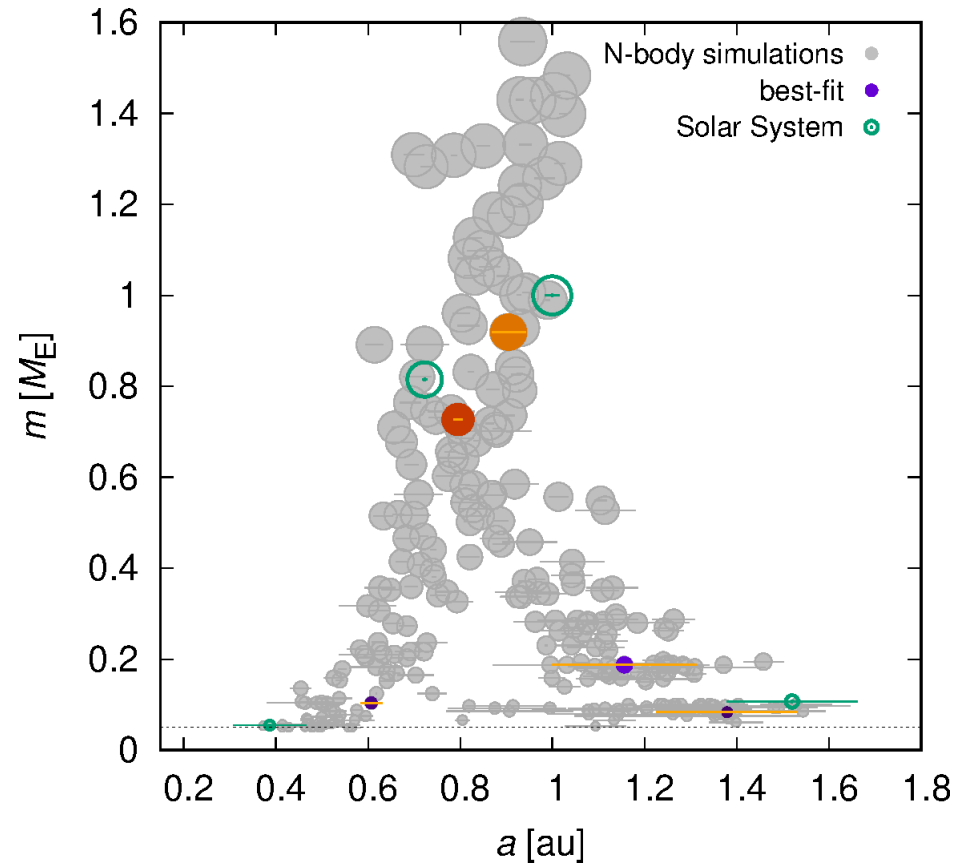
Simulace se srážkami

- konvergentní zóna → malá tělesa na okraji, tj. Merkur & Mars

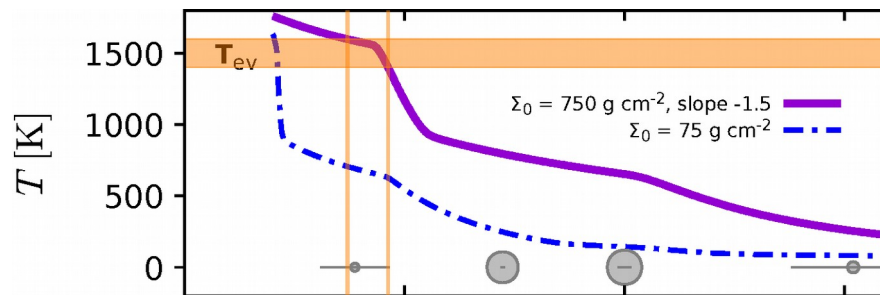


Statistika TP

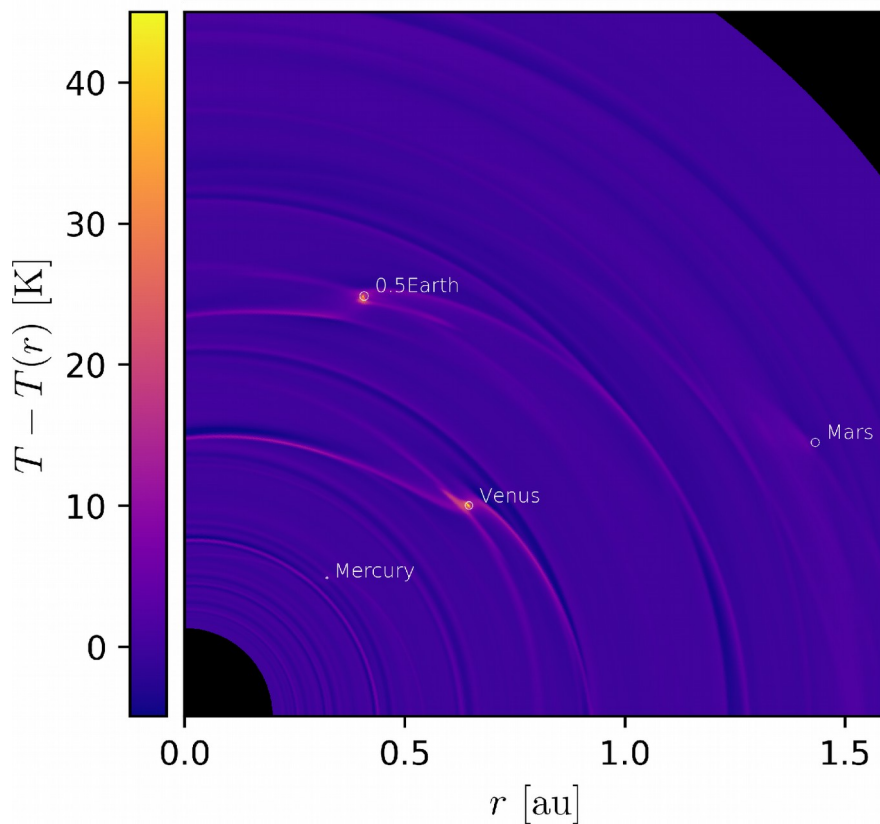
- malá vzdálenost mezi Venuší a Zemí (0.3 au; cf. Deienno et al. 2019)



profil $T(r)$, z počátku
horký vnitřní okraj?

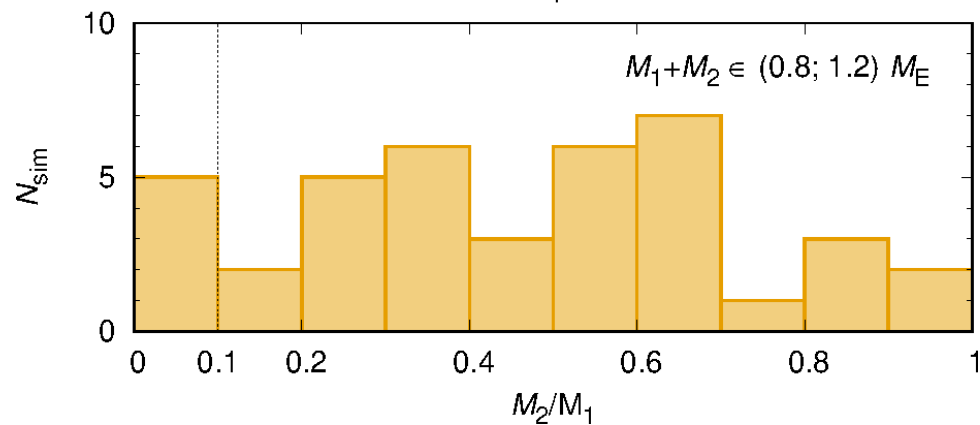
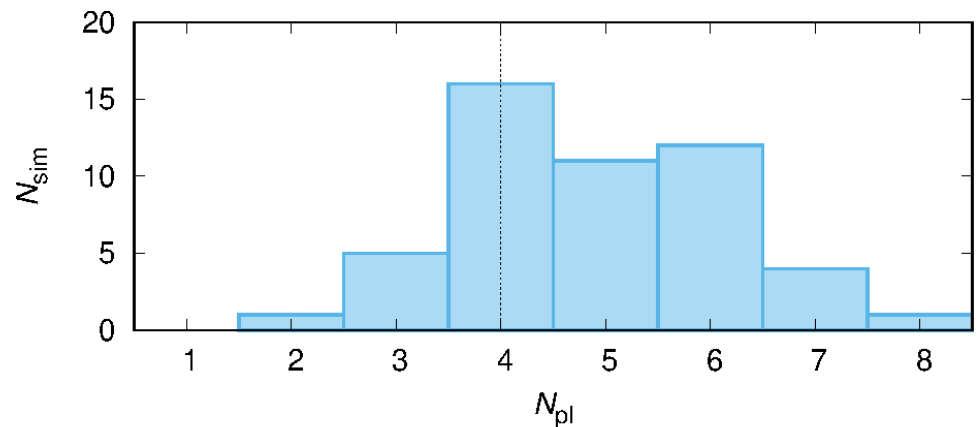


perturbace $T(x, y)$;
jev horké stopy



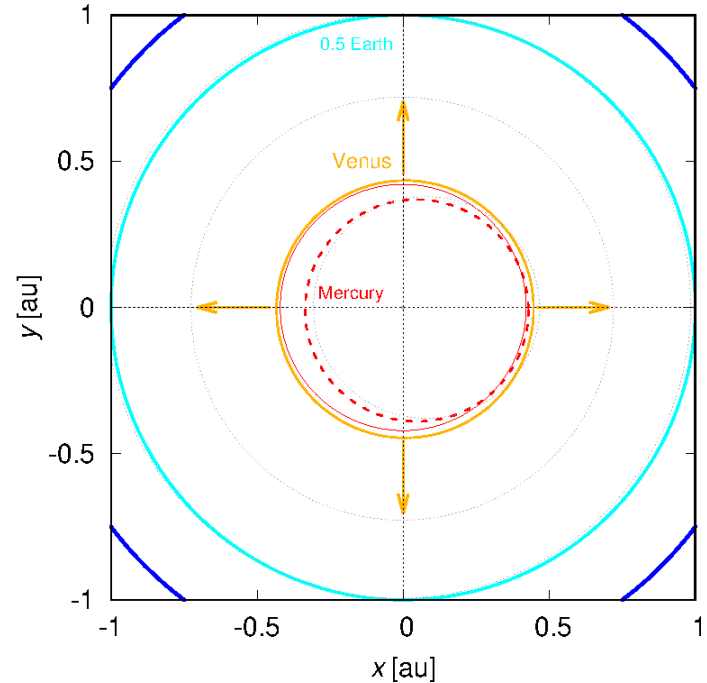
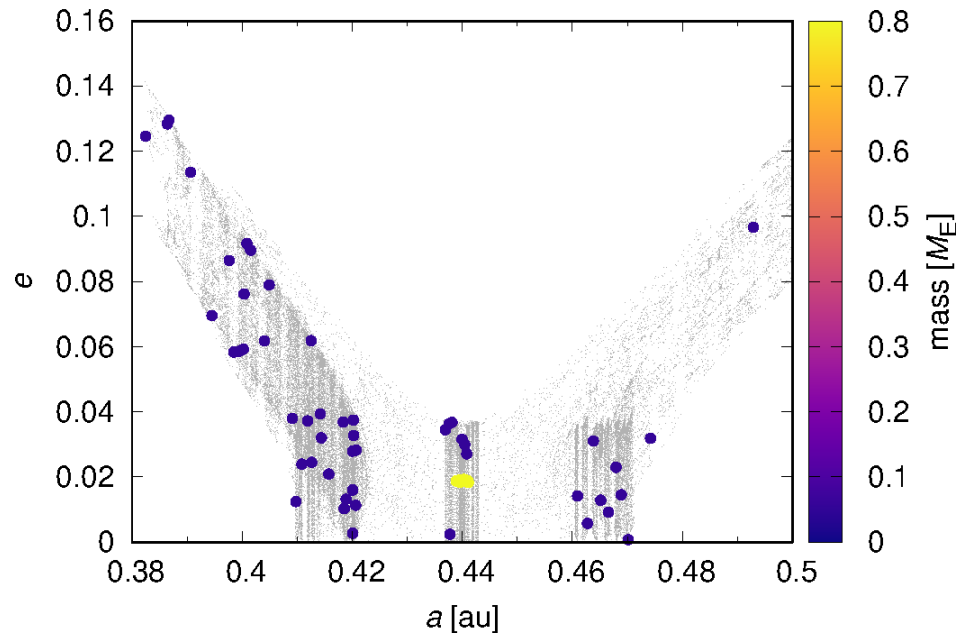
Počet planet

- 4-6 planet
- impakty 0.5/0.5-Země stejně časté jako kanonické!



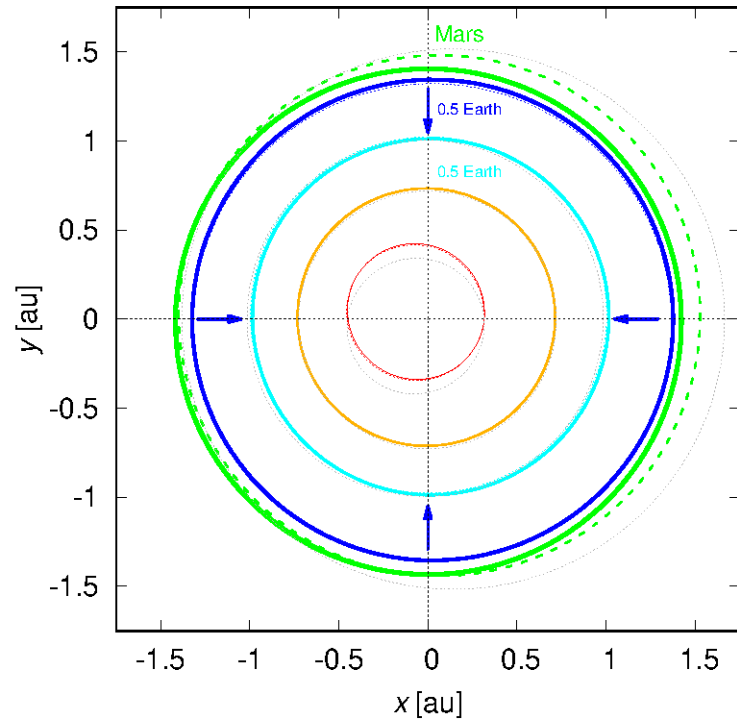
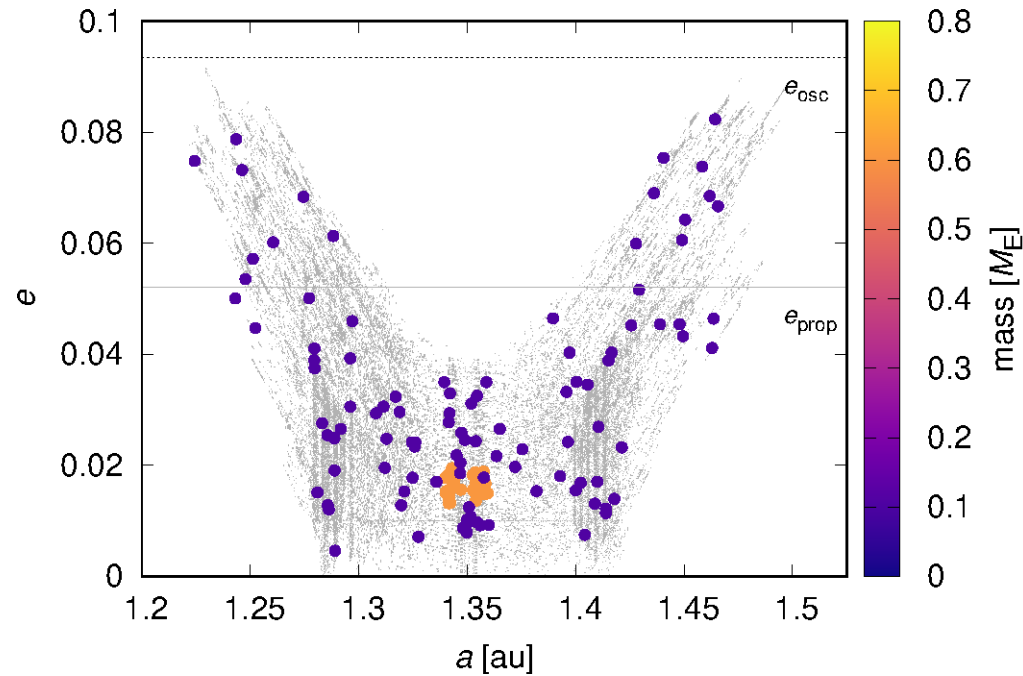
Rozptyl Merkuru na Venuši

- excentricita Merkuru; oddělení drah RHD (mirace, tlumení), jinak pouze srážky



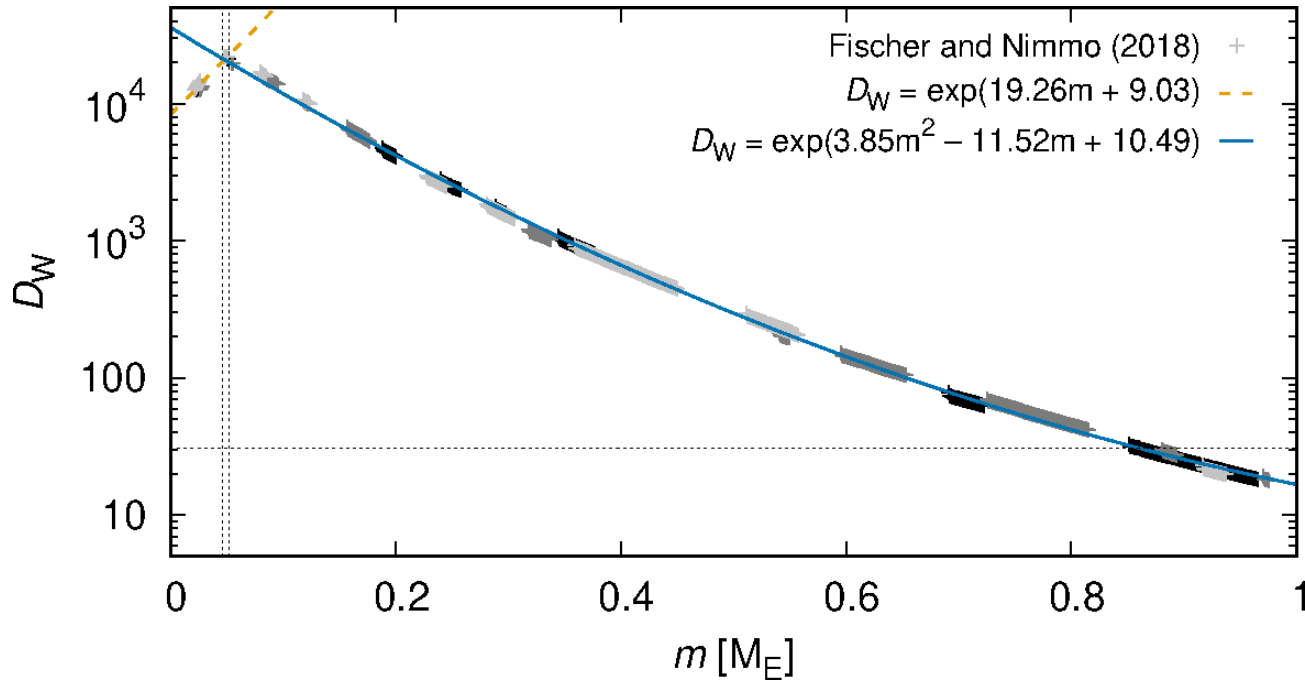
Rozptyl Marsu na 0.5-Zemi

- dtto pro Mars, $|da/dt|$ pro 0.5-Zemi $>$ Mars



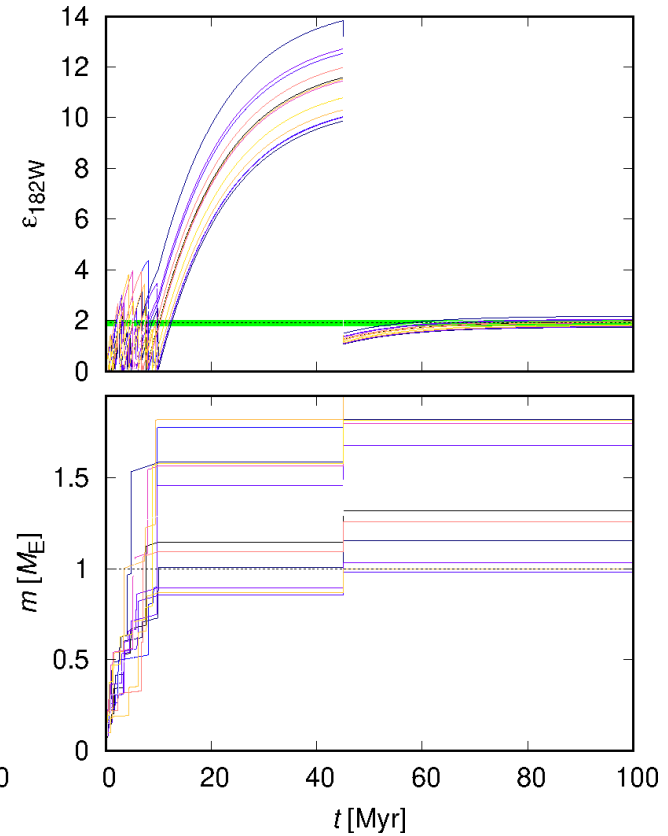
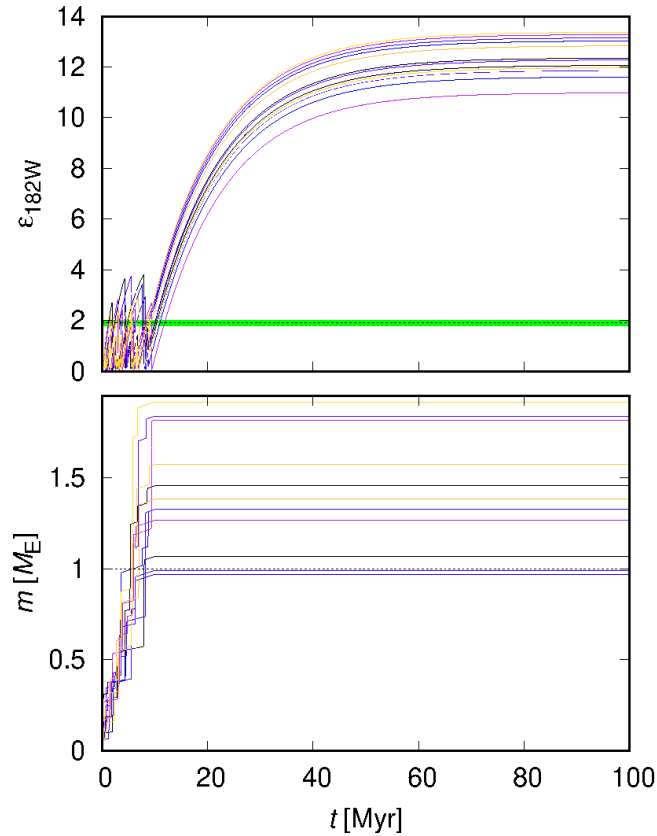
Rozdělovací koeficient D_W

- Fischer & Nimmo (2018)



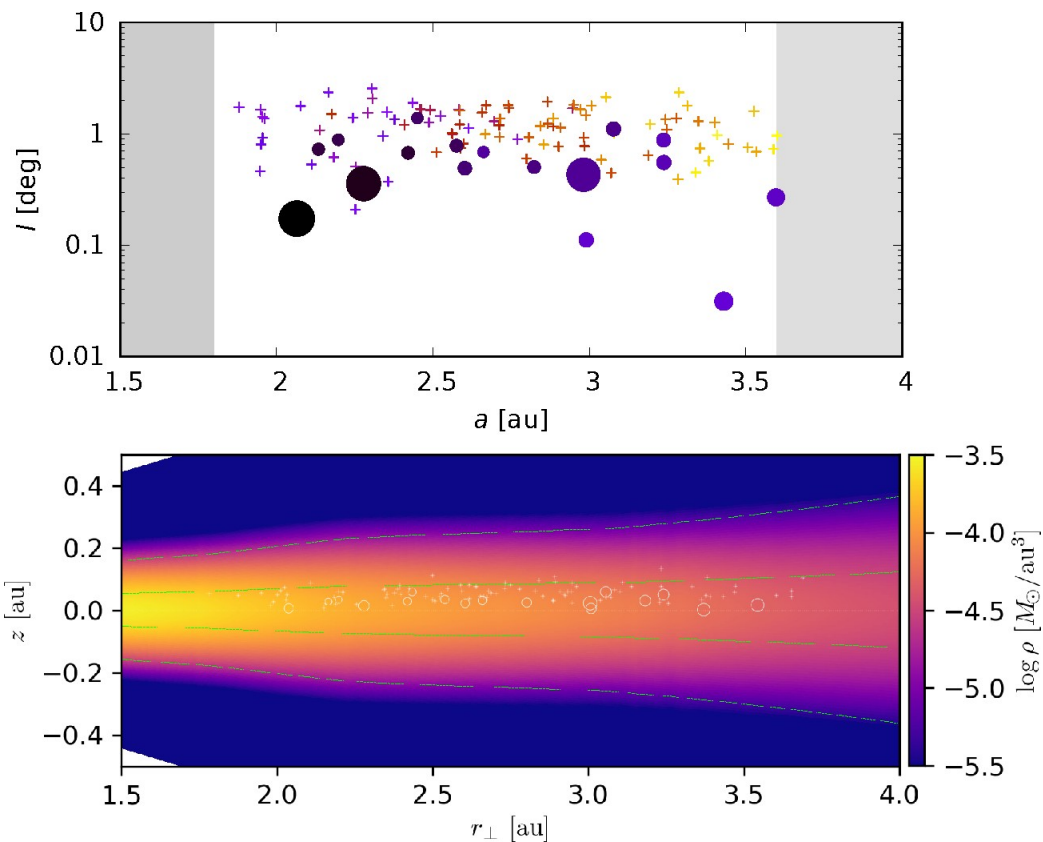
Anomálie ^{182}W

- Yu & Jacobsen (2011)



Hlavní pás asteroidů v disku

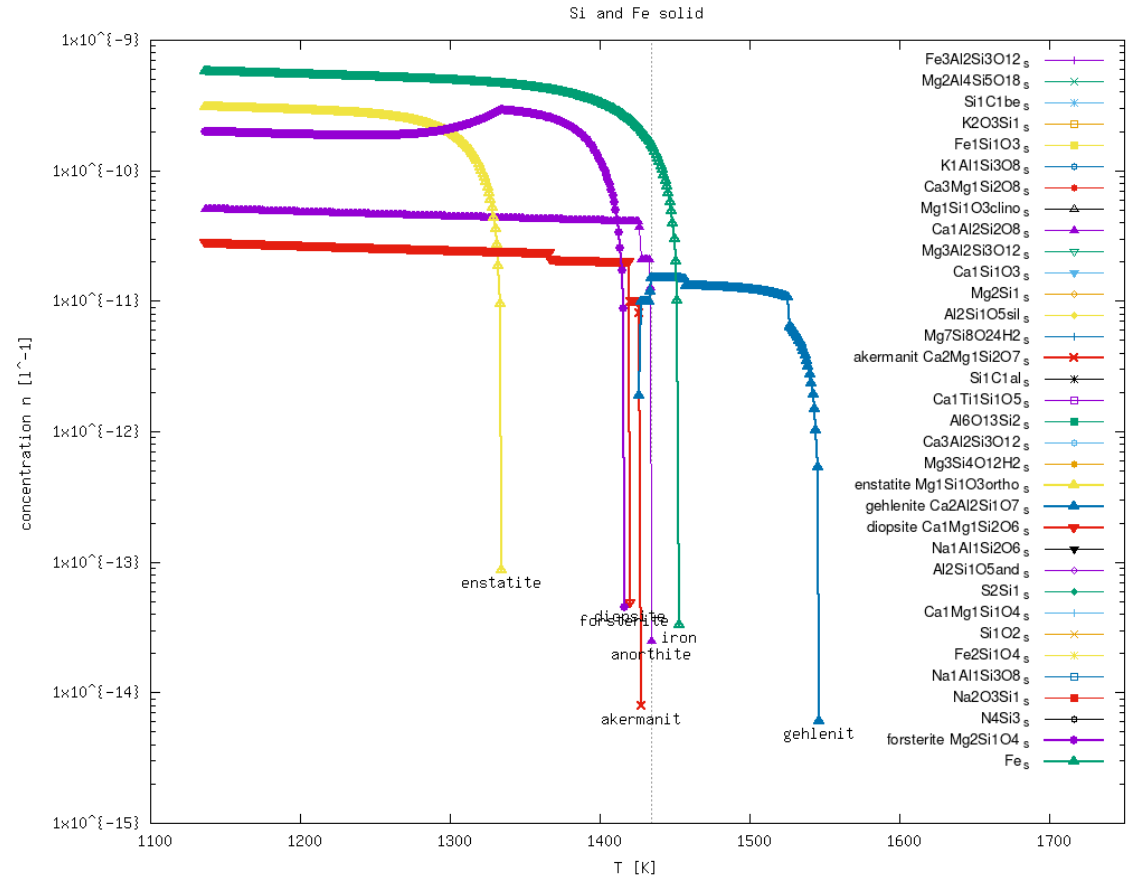
- sněžná čára = **divergentní zóna** (Bitsch et al. 2014)
- migrace embryí → excitace asteroidů & tlumení plynem



Kondenzační sekvence

- Unterborn & Panero (2017)
- chemický kód ArCCoS
- žádný drift balvanů, ale...
- ... pokud je obohacení o Fe a enstatit/forsterit → Fe/Si pro **jádro Merkuru**

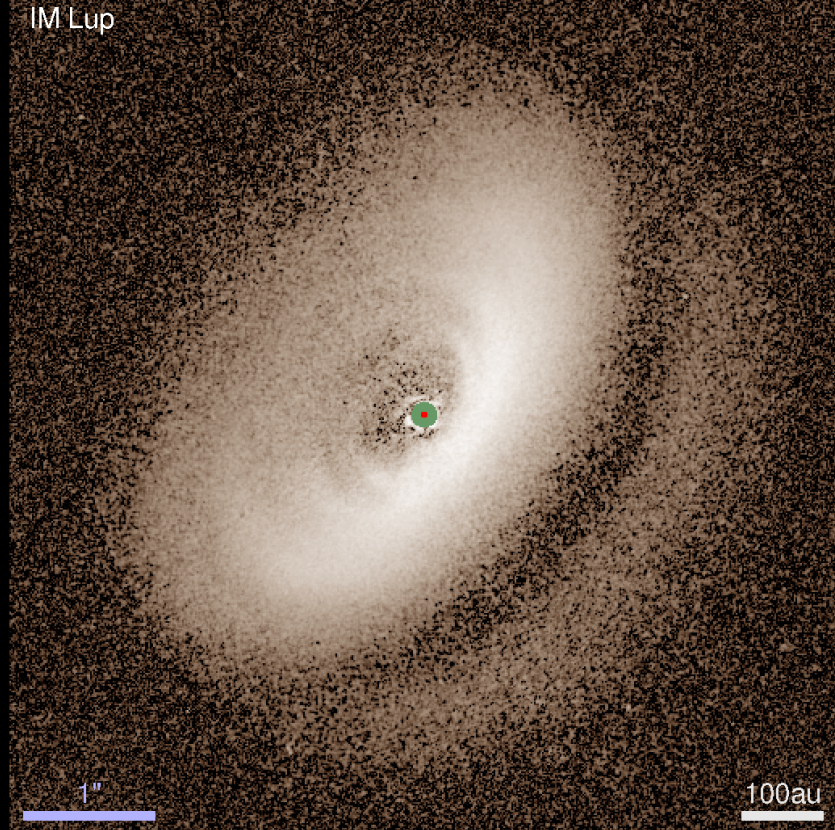
cf. Asphaug & Reufer (2014)



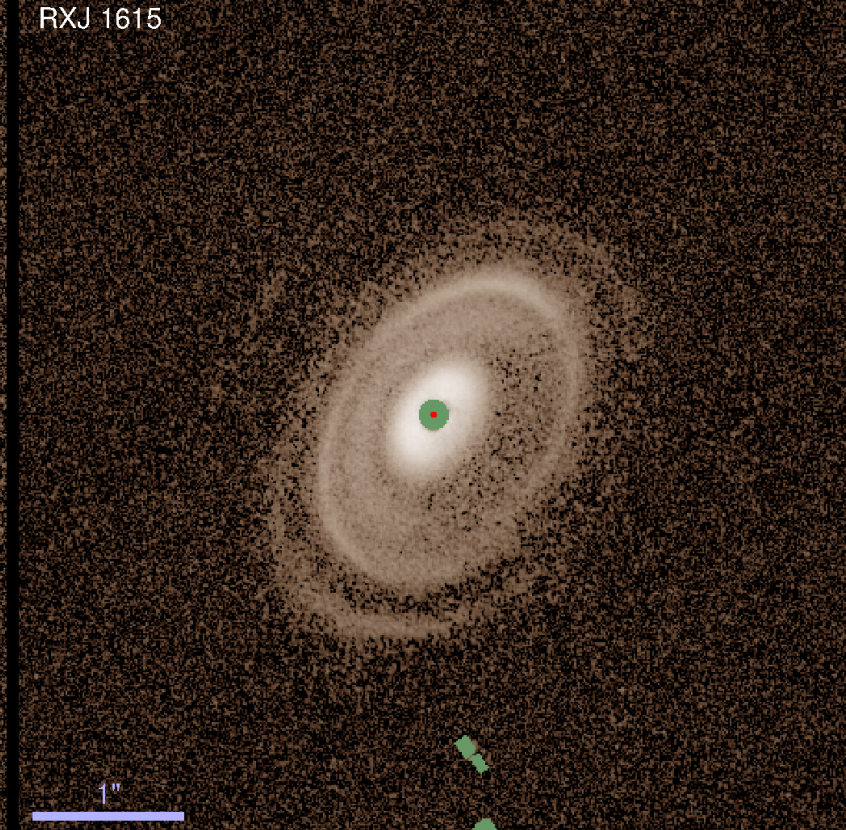
Další implikace...

- transport vody
- vnitřní okraje disků (0.1 au)?!
-

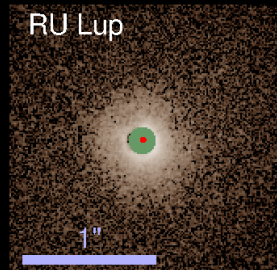
IM Lup



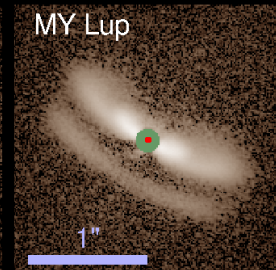
RXJ 1615



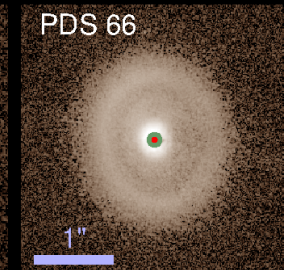
RU Lup



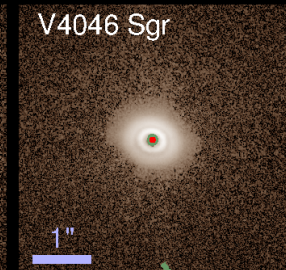
MY Lup



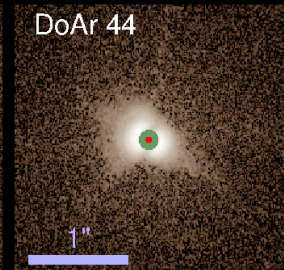
PDS 66



V4046 Sgr



DoAr 44



AS 209

